Mechanical Behavior of Steel Pipe Bends; An Overview.

Citation for published version:
Karamanos, S 2016, 'Mechanical Behavior of Steel Pipe Bends; An Overview.' Journal of pressure vessel technology-Transactions of the asme, vol. 138, no. 4, 041203. DOI: 10.1115/1.4031940

Digital Object Identifier (DOI):
10.1115/1.4031940

Published In:
Journal of pressure vessel technology-Transactions of the asme

MECHANICAL BEHAVIOR OF STEEL PIPE BENDS; AN OVERVIEW[1]

Spyros A. Karamanos
Department of Mechanical Engineering
University of Thessaly, Volos 38334, Greece
email: skara@mie.uth.gr

Abstract

An overview of the mechanical behavior of steel pipe (elbows) is offered, based on previously reported analytical solutions, numerical results and experimental data. The behavior of pipe bends is characterized by significant deformations and stresses, quite higher than the ones developed in straight pipes with the same cross-section. Under bending loading (in-plane and out-of-plane) the main feature of the response is cross-sectional ovalization, which influences bending capacity and is affected by the level of internal pressure. Bends subjected to cyclic in-plane bending exhibit fatigue damage, leading to base metal cracking at the elbow flank. Using advanced finite element tools, the response of pipe elbows in buried pipelines subjected to ground-induced actions is also addressed, with emphasis on soil-pipeline interaction. Finally, the efficiency of special-purpose finite elements for modelling pipes and elbows is briefly discussed.

1. Introduction

Pipe bends, often referred to as elbows, are curved pipe parts widely used in piping systems of industrial plants or power stations (Figure 1a). Their mechanical behaviour, compared with straight pipe segments, is significantly more flexible and associated with significantly higher stresses and strains, and very pronounced cross-sectional deformation, referred to as "ovalization". Because of their flexibility, they can accommodate thermal expansions and absorb other externally-induced loading, but they are considered as critical components for the structural integrity of piping systems. For the case of extreme loading conditions, their mechanical response is characterized by a biaxial state of stress and strain, which may lead to pipe elbow failure, in a mode quite different than the one expected in straight pipes.

[1] This paper has been prepared for the JPVT 50th Anniversary Issue

Pipe elbows in industrial piping systems have relatively small radius of bend curvature R with respect to pipe diameter D (Figure 2). In ASME 16.9 standard (ASME, 2007), pipe elbows of diameter ranging from ½ to 48 inches are specified, and the ratio of the longitudinal radius R over the pipe diameter D is equal to either 1 ("short radius" bends) or 1.5 ("long radius" bends). Similar pipe elbow dimensions are specified in the relevant European standard EN 10253-1.


(a)

(b)

Figure 1. Pipe elbows (bends) in (a) piping systems of industrial plants; (b) buried gas pipelines.

For the case of large-diameter steel hydrocarbon transmission pipelines, pipe elbows or bends are used to accommodate the pipe in the direction of pipeline alignment (Figure 1b). Large-diameter pipeline bends can be either "hot" or "cold" bends. Cold pipe bends, sometimes referred to as "field bends", are manufactured at the construction site from straight pipes, with the use of special bending devices, and are commonly employed in pipeline construction practice. For typical large-diameter pipes (i.e. from 36 to 56 inches), the R/D ratio of the bend radius R over the pipe diameter D may range between 30 and 45. In the case of abrupt changes of pipeline direction, small-radius "hot bends" are also employed, usually manufactured through induction heating and bending; a typical value of the R/D ratio for those hot bends is equal to 5, which allows for pigging inspection operations in the course of pipeline maintenance.

The present paper offers an overview of the response of steel pipe bends (elbows) under structural loading, in the presence of pressure, in an attempt to identify and summarize their main features of mechanical behavior and the corresponding principal failure modes under various loading conditions. In section 2, some important features stemming from the small-strain elastic analysis of pipe elbows subjected to in-plane and out-of-plane bending are presented. The behavior of pipe bends under severe monotonic loading is presented in section 3, whereas in section 4 the response of pipe bends under strong cyclic loading is discussed; in both sections, reference to experimental results is made. The particular case of bends in buried pipelines under ground-induced actions is briefly discussed in section 5, addressing the issue of soil-pipeline interaction and presenting some novel results. In section 6, an overview of special-purpose elements are described, suitable for the efficient modelling of elbows in piping systems. Finally, some important conclusions from the previous sections are summarized in section 7.

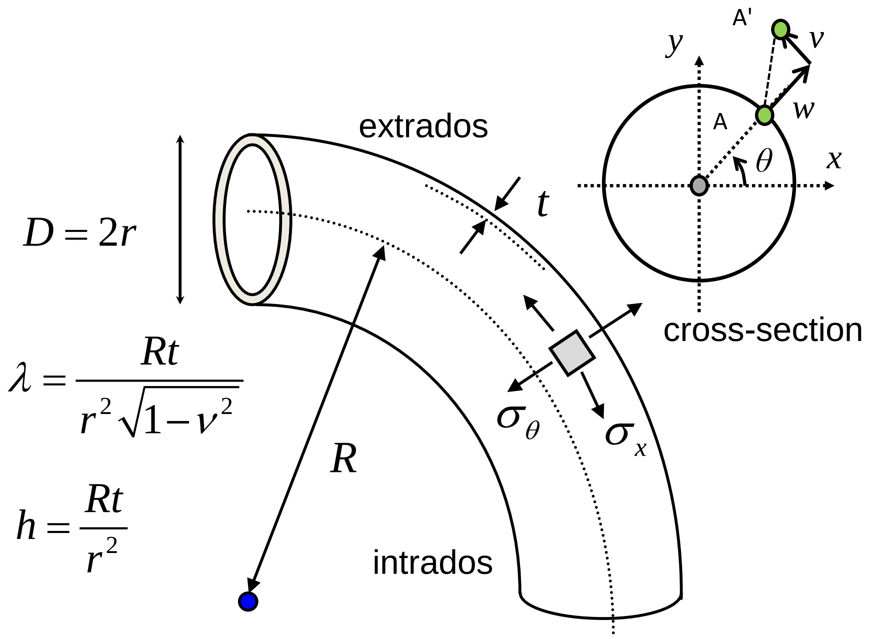

Figure 2. Pipe elbow geometry, cross-sectional displacements and biaxial state of stress.

2. Small-Strain Elastic Behavior

The stress analysis of piping systems and pipelines constitutes an essential part of pipe design procedure under operating loads. In this design process, elbows (bends) are considered as critical components, exhibiting significantly higher stresses, deformations and bending flexibility than straight pipes of the same cross-sectional properties. The configuration of a typical elbow, widely employed in piping systems, is shown in Figure 2. The geometry is characterized by the pipe diameter D, the pipe thickness t, the bend radius R, and is usually expressed through by the dimensionless parameters λ or h, also defined in Figure 2. Parameter λ arises in analytical calculations, as the ones described briefly below, and parameter h is often employed in design standards, such as the ASME B31 standards (ASME, 2010a; 2010b) or EN 13480-3 (CEN, 2002).

The early analytical work of Von Karman (1911) can be used for understanding the particular mechanical behavior of pipe bends. Von Karman, employed a simple two-dimensional formulation that couples longitudinal strain energy due to bending, with hoop strain energy due to ovalization, assumes inextensional ring theory, and considers a simple doubly-symmetric trigonometric function for the radial displacement of arbitrary point of the elbow cross-section w, shown in Figure 2:

$$w(\theta) = \alpha \cos 2\theta \qquad (1)$$

Minimization of the strain energy results in the following expression for the moment-curvature relationship in the absence of internal pressure, written below in a non-dimensional form:

$$m = \pi\kappa\left(1 - \frac{9}{10 + 12\lambda^2}\right) \qquad (2)$$

where m and κ are the dimensionless values of moment M and curvature k, normalized by $M_e = Ert^2 \big/ \sqrt{1-\nu^2}$ and $k_N = t \Big/ \left(r^2\sqrt{1-\nu^2}\right)$ respectively. The elbow geometry is expressed in terms of the dimensionless elbow parameter λ (see Figure 2). From equation (2), one may readily obtain the flexibility factor η, defined as the ratio of elbow bending flexibility over the flexibility of the corresponding straight pipe, as follows:

$$\eta = \left[1 - \frac{9}{10 + 12\lambda^2}\right]^{-1} \qquad (3)$$

A more enhanced energy formulation can be employed to describe in more detail the mechanical behavior of elastic elbows, proposed by Rodabaugh and George (1957), including the effects of internal pressure. This formulation is a generalization of the Von Karman (1911) solution. It assumes uniform cross-sectional deformation along the elbow axis, and the total potential energy of the bent and pressurized elbow is written in terms of the radial and the tangential displacements of the arbitrary point A, denoted w, v respectively as shown in Figure 2, which are discretized through series of doubly-symmetric trigonometric functions and the corresponding generalized coordinates a_n:

$$v(\theta) = \sum_{n=1}^{\infty} a_n \sin 2n\theta \qquad (4)$$

$$w(\theta) = -\sum_{n=1}^{\infty} 2a_n \cos 2n\theta \qquad (5)$$

Solution is obtained by minimization of the potential energy, and the results are expressed in terms of the flexibility factor η. Furthermore, the longitudinal and hoop stresses, and the ovalization of the cross-section are also computed. Despite the fact that this solution has been presented in the late 50's, it still constitutes the basis of current pipe design specifications, such as the ASME B31 standards (ASME, 2010a, 2010b) or EN 13480-3 (CEN, 2002). The main outcome of the above analyses is that the response is governed by cross-sectional ovalization, shown schematically in Figure 3; under in-plane bending, the elbow flattens in an oval shape symmetric with respect to the plane of bending for closing or opening bending. However, the flattening pattern under opening moments is opposite to the one that occurs under closing moments; the pattern observed in opening moments is referred to as "reverse ovalization" and plays a significant role in the mechanical response of elbows. In the case of out-of-plane bending, cross-sectional flattening occurs at 45-degrees with respect to the plane of bending.

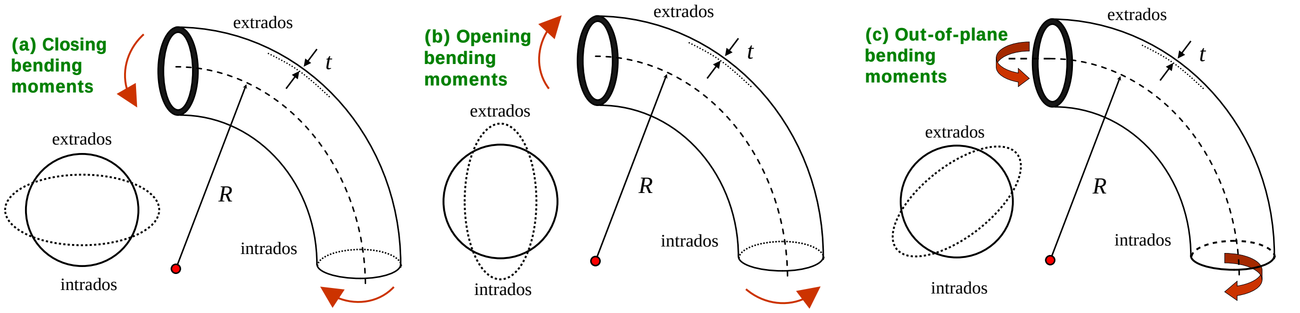

Figure 3. Schematic representation of ovalization in (a) in-plane closing moments; (b) out-of-plane opening moments "reverse ovalization"; (c) out-of-plane bending.

Figure 4 presents the flexibility factor in terms of dimensionless parameter λ, and the pressure level in the pipe elbow. Pressure is expressed in terms of the dimensionless pressure parameter $\psi = pR/Ert$. The flexibility values of Figure 4 indicate that the curved pipe (elbow) is substantially more flexible than the corresponding straight pipe. The flexibility factor is higher in the absence of internal pressure and is reduced when internal pressure is raised. Figure 5 depicts the longitudinal and the circumferential stresses around the pipe cross-section, assuming elastic behavior of the elbow material, as a function of the distance y from the pipe axis. The elbow under consideration has outside diameter D=165 mm, thickness t=3 mm and R/D ratio equal to 3, subjected to a bending moment equal to 10 kN-m. It is interesting to note that the maximum circumferential stress is higher than the maximum longitudinal stress. Furthermore, the maximum longitudinal stress is considerably higher than the maximum stress of a straight pipe with the same cross-section, and does not occur at the top or the bottom of the cross-section. Cross-sectional ovalization is the main reason for this behavior.

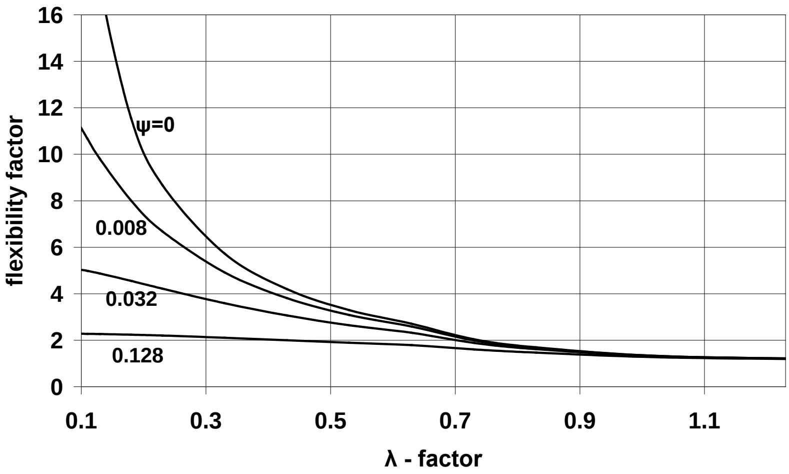

Figure 4. Flexibility factor of pipe elbows with respect to the elbow parameter λ.

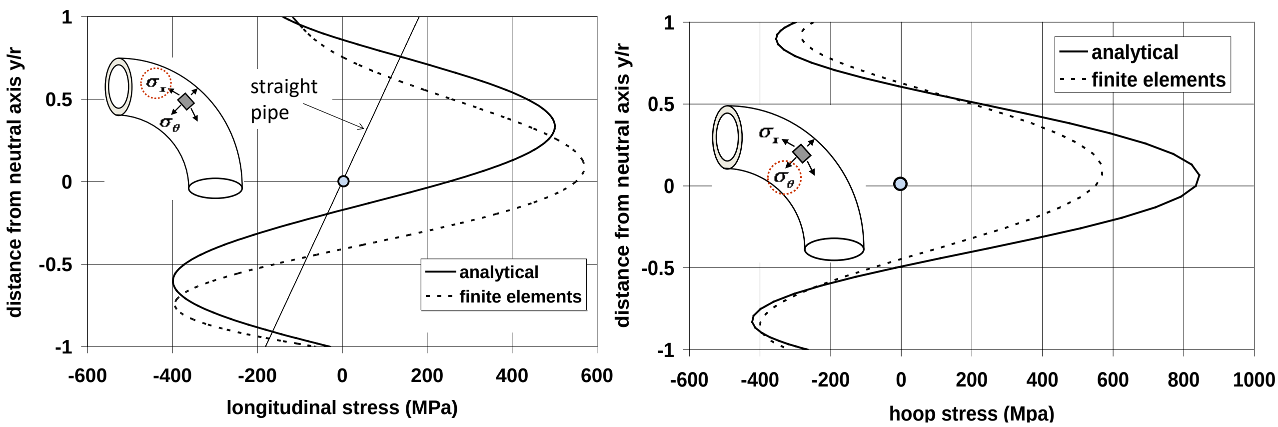

Figure 5. Elastic analysis of a 90-deg standalone elbow (λ=0.23); variation of (a) longitudinal stresses and (b) hoop stresses at external pipe wall with respect to the cross-sectional height; comparison of the analytical solution of Rodabough & George (1957) with finite element results.

The above observations clearly show the special features of pipe bend behavior; it is substantially different than the behavior of a straight pipe, in terms of both stiffness and stress. One should notice though, that the above analysis has several limitations: it assumes elastic material response, small displacements and constant curvature along the pipe. Those assumptions are discussed below.

In practical applications, elbows are connected to straight pipe segments, resulting in a variation of deformation and ovalization along the elbow, with the maximum deformation in the middle cross-section of the elbow, and the assumption of constant curvature along the bend is not applicable. In such a case, a numerical simulation is required. Figure 6 shows a set-up used for in-plane and out-of-plane bending loading of a 90-degree pipe elbow, with diameter D=160 mm, thickness t=3 mm. The response of this pipe, subjected to in-plane closing bending moments for different levels of pressure, is shown in Figure 7. The results show the increase of stiffness with increasing level of internal pressure, and the experimental results are compared quite successfully with numerical results from a finite element model that employ shell elements and simulate the experimental procedure of Figure 6 (Karamanos *et al.*, 2006).

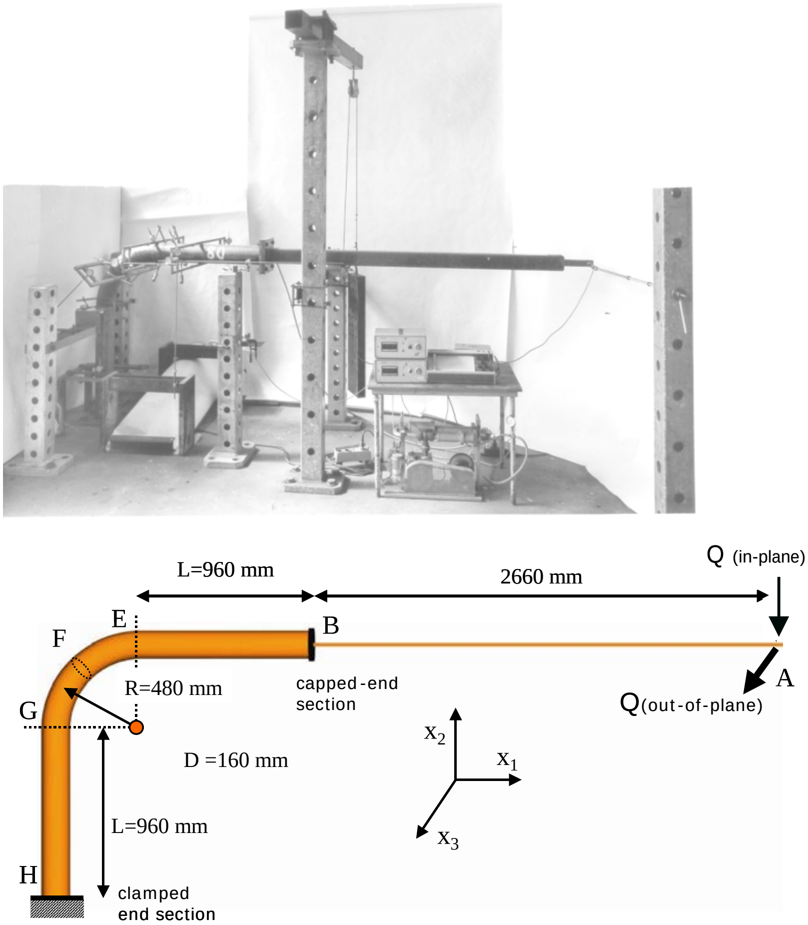

Figure 6. (a) Experimental set-up for testing a 160-mm-diameter pipe elbow under in-plane and out-of-plane bending; (b) Schematic representation of the 90 deg specimens (Karamanos *et al.*, 2006).

Furthermore, the assumptions of elastic material behavior and small displacements are valid only for low levels of loading, associated with operational loading conditions. In the case of severe loading conditions, e.g. in the course of a strong seismic event, the elbow behavior at the ultimate limit state is characterized by large displacements and significant inelastic material deformations. To predict numerically the mechanical behavior of steel elbows under severe loading conditions, a numerical simulation that considers geometric and material nonlinearities is necessary. It is noted that an analysis of pipe elbows with only material nonlinearities may not be appropriate for obtaining reliable results; cross-sectional distortion is quite significant and the ensuing geometric nonlinearities due to large displacements should be taken into account in the analysis.

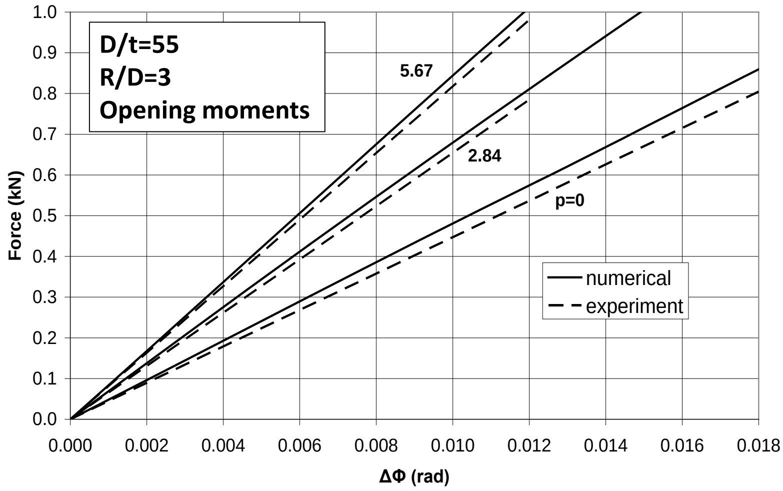

Figure 7. Elastic flexibility of pipe elbow specimen (*D/t*=53.3, *R/D*=3) under in-plane closing bending moments; comparison between numerical and experimental results (values of pressure p are in MPa).

3. Behavior under severe monotonic loading

Previous works (e.g. Shalaby and Younan, 1998; Karamanos *et al.* 2003, 2006) have pointed out that under severe loading conditions the development of significant cross-sectional ovalization is associated with the development of significant stresses and strains both in the circumferential and the longitudinal direction. In addition, it has been recognized that the response under closing bending moments is substantially different than the response under opening bending moments. This is mainly due to the different sign of ovalization due to opening bending moments, referred to as "reverse ovalization", described in the previous section and depicted in Figure 3c; this reverse ovalization increases cross-sectional height and results in higher bending moment capacity.

Sobel and Newman (1980, 1986), and Dhalla (1987) reported experiments on the bending response of elbows through a series of tests on 16-inch-diameter 90 deg elbows (D/t=39 and R/D=1.5) under in-plane closing moments. The test data were compared with numerical results from shell elements and simplified elbow elements. Gresnigt et al. (1985, 1986) reported test data on five 30 deg, five 60 deg and one 90 deg steel elbows (R/D=3) under bending and pressure. The 30 deg and 60 deg specimens were tested under inelastic in-plane bending, whereas the 90 deg specimen was subjected to out-of-plane bending. An analytical model for the elastic-plastic cross-sectional deformation of elbows was also developed by Gresnigt *et al.* (1986, 1995), introducing a correction factor to account for the influence of the adjacent straight pipe segments. Greenstreet (1978) investigated experimentally the response of carbon steel and stainless steel pipe elbows, under in-plane and out-of-plane bending loading conditions, in the presence of internal pressure. Hilsenkopf *et al.* (1988) reported test data on thin-walled (D/t=89.5) stainless steel elbows and thick-walled (D/t=13.4) ferritic elbows under both in-plane and out-of-plane bending, in connection with their functional capability. Suzuki and Nasu (1989) conducted two in-plane closing moment tests on a 12-inch 90 deg elbow (D/t=46.3) and on a 24-inch 90 deg elbow (D/t=64.9) and compared the test data with numerical predictions from four-node shell elements. More recently, Tan *et al.* (2002) reported one closing in-plane moment test and one opening in-plane moment test on 90 deg thick stainless steel elbows (D/t=10.5) and compared their measurements with finite element analysis results.

The development of computational methods (e.g. finite elements) enabled the numerical investigation of elbow response and the prediction of ultimate capacity. To model elbow deformation at the ultimate limit state, a nonlinear analysis accounting for both material and geometric nonlinearities is necessary. Using the special-purpose "elbow" element ELBOW31B of ABAQUS, Shalaby and Younan (1998, 1999) analyzed standalone 90 deg steel elbows (R/D=1.5) for a wide range of diameter-to-thickness ratios ($15.5 \leq D/t \leq 97$), under in-plane bending (opening and closing moments) and internal pressure. In subsequent papers, Mourad and Younan (2001, 2002) analyzed pressurized standalone 90 deg steel elbow segments (R/D=1.5) under out-of-plane bending for a wide range of diameter-to-thickness ratios ($15.5 \leq D/t \leq 97$), using special-purpose "elbow" element ELBOW32 of Abaqus software. In those investigations, only the curved part of the pipe was analysed, neglecting the effects of the adjacent straight parts. Chattopadhyay *et al.* (2000) employed general-purpose program NISA to analyze thick 90 deg elbows (*D/t*≤25) under in-plane bending, through twenty-node fully-integrated solid elements, accounting for the effects of the adjacent straight parts. Using a curve-fitting procedure, simplified formulae were proposed for the collapse (limit) moment capacity in terms of pressure and the bend factor *h*. Karamanos *et al.* (2003) have presented a numerical study of steel elbow response under in-plane bending. Emphasis was given on the buckling failure of non-pressurized thin-walled elbows, and a good comparison was found between numerical results and test measurements reported by Gresnigt et al. (1985, 1986). In a subsequent work, Karamanos *et al.* (2006) extended the work of Karamanos *et al.* (2003), and focused on the ultimate capacity of 90 deg steel elbows under pressurized bending (in-plane or out-of-plane). The study was based on simulation of elbows with nonlinear elastic-plastic shell finite elements, supported by experimental results. The numerical results have been compared with experimental measurements from a 90 deg elbow reported by Gresnigt et al. (1985, 1986). A parametric study has also been conducted to investigate the pressurized bending response of three 90 deg elbows (D/t=90, 55, 20). The ultimate moment capacity of the elbows and the corresponding failure modes has been identified, with emphasis on buckling. Furthermore, the effects of internal pressure on the ultimate bending resistance have been extensively investigated and discussed, and special attention has been given on the out-of-plane bending response, in terms of the ultimate bending moment and the corresponding failure mode.

It is interesting to note that the majority of the work published on the ultimate bending moment capacity of pipe bends refers to in-plane bending moments, whereas the out-of-plane bending capacity has received significantly less attention. The out-of-plane bending experiments reported by Gresnigt *et al.* (1985, 1986), Greenstreet (1978) and Hilsenkopf *et al.* (1988) indicated that, under this type of loading, 90 deg elbows are capable of undergoing significant inelastic deformation, before collapse, and that the ultimate moment capacity is affected by the presence of internal pressure. The same observations have been noticed in relevant numerical investigations (Mourad and Younan, 2001, 2002; Karamanos *et al.* 2006).

The response of a 60-degree elbow subjected to in-plane closing and opening bending moments is shown in Figure 8, in terms of the corresponding moment-rotation diagrams. The experimental set-up is schematically shown in Figure 9, where bending moments are applied through special devices at the end sections of the straight pipe segments, as reported by Karamanos *et al.* (2003). The deformed shapes of the elbows are shown in

Figure 10. The pipe elbows have diameter equal to 261 mm, thickness equal to 2.9 mm, material, and bend radius R=772 mm, corresponding to R/D ratio equal to 3. In the case of closing bending moments, the response is characterized by excessive ovalization, with cross-sectional flattening perpendicular to the plane of bending. Failure of the pipe bend occurs due to the development of excessive flattening and the development of high strains at the "flank" of the central elbow cross-section, as shown in Figure 10a. On the other hand, the response under opening moments is quite different; significant ovalization develops, which flattens the pipe cross-section in the direction of the bending plane ("reverse" ovalization), and the failure mode of the elbow is local buckling at the central cross-section of the elbow, at a location between the flank and the extrados, as shown in Figure 10b. The results from the numerical simulations with shell elements, shown in Figure 8 (Karamanos *et al.*, 2003) and in Figure 11, are in very good agreement with the experimental results in terms of the corresponding moment-rotation diagrams and the corresponding deformed shapes.

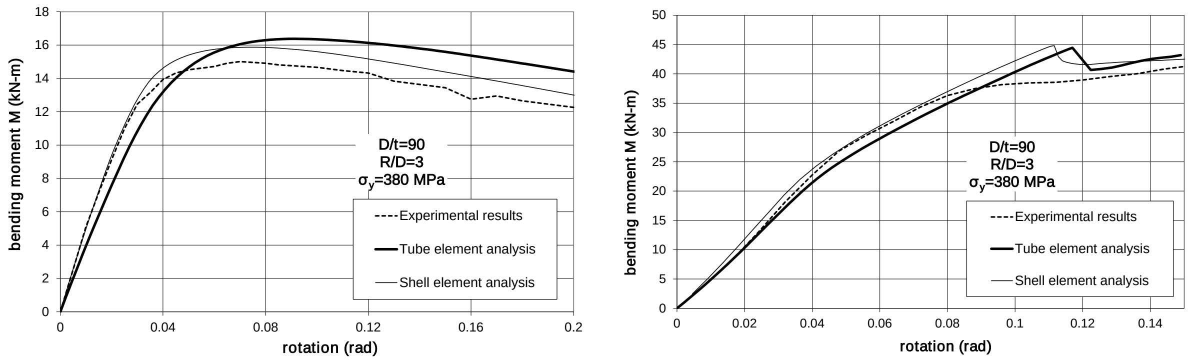

Figure 8. Moment-rotation diagrams for non-pressurized 60 deg elbows (D/t=90); comparison between test data and numerical results (Karamanos *et al.* 2003).

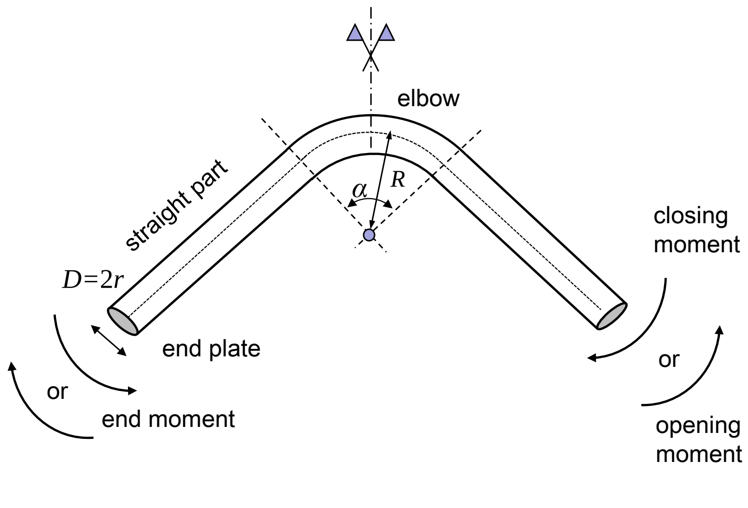

Figure 9. Schematic representation of elbow experiments (Karamanos *et al.* 2003).

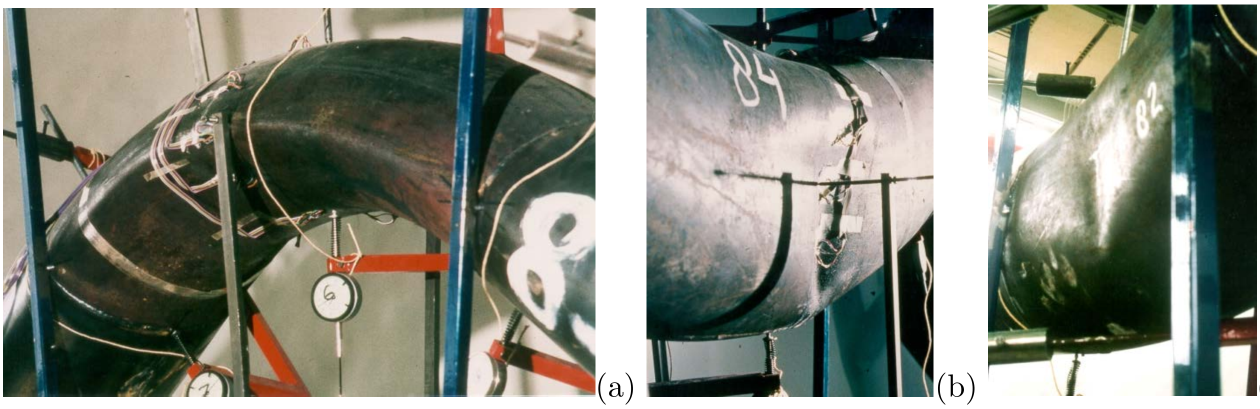
(a) (b) (c)

Figure 10. Deformed shapes of 60 deg elbows (D/t=90); (a) flattened configuration under closing moments and (b), (c) buckled shape under opening moments (Karamanos *et al.* 2003).

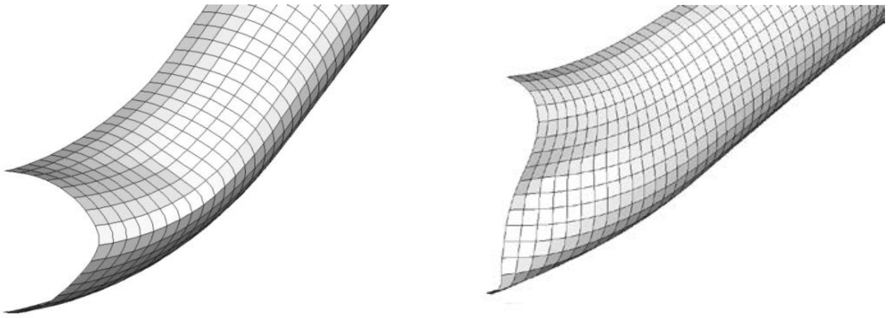

Figure 11. Finite element simulation of 60 deg elbow deformation under in-plane closing bending (D/t=90); (a) ovalized shape under in-plane bending moments (b) buckled shape under opening bending (Karamanos *et al.* 2003).

The effect of internal pressure on pipe elbow response is depicted in Figure 12 for a 30-degree elbow with diameter equal to 160 mm, thickness 2.9 mm, bend radius of 480 mm, pressurized to 8.77 MPa (60% of the nominal yield pressure, $p_y = 2\sigma_y t/D$) reported by Karamanos *et al.* (2003). The presence of internal pressure has a positive effect on the bending capacity, allowing for significant deformation (rotational) capacity without fracture, i.e. with "no loss of containment", provided that the steel material has adequate ductility.

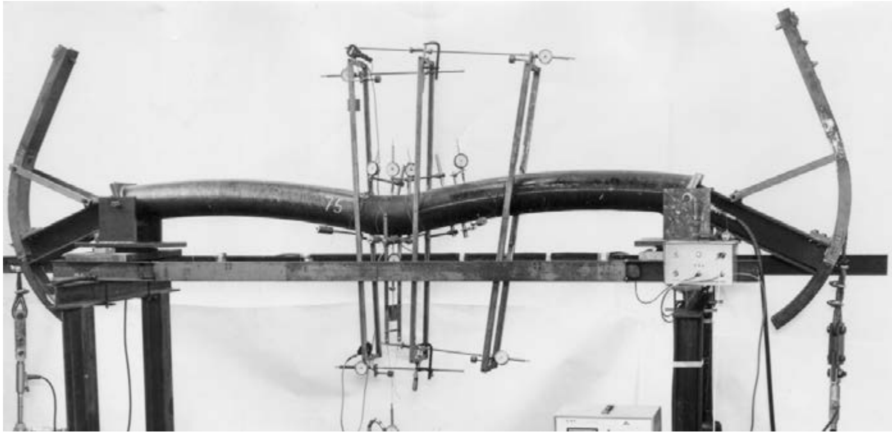

Figure 12. Final configuration of a pressurized 30 deg elbow specimen (*D/t*=55) subjected to opening bending moments.

The response of a thin-walled 90-degree elbow under in-plane bending is shown in Figure 13a and Figure 13b for closing and opening bending moments respectively. The pipe elbows have diameter *D*=270 mm, thickness *t*=3 mm (*D/t*=90) and bend radius *R*=480 mm. The results are obtained from numerical simulations that employ shell elements. In Figure 13 moment-rotation diagrams are reported and show a dramatic difference between closing and opening bending (Karamanos *et al.*, 2006), also noted in the elbow results of Figure 8. A first observation refers to the bending moment capacity under zero internal pressure; the ultimate closing moment is less than 20% of the full-plastic bending moment of the pipe cross-section $M_P = \sigma_y D^2 t$. Most of the deformation occurs at the two flank locations, due to cross-sectional flattening, associated with the development of high local strains in the hoop direction, and the elbow fails due to excessive ovalization, shown in Figure 14, a mode also observed in Figure 10a. On the other hand, for the case of opening bending moments the critical moment is about 50% of the full plastic moment. At that stage, the elbow exhibits local buckling at the central section, similar to the one depicted in Figure 10b.

The effect of internal pressure has a significant effect on bending response for the 90-degree thin-walled pipe bend under consideration, as shown in Figure 13. Apart from the increase of bending stiffness, in the first stages of loading, the corresponding bending moment is also increased; this beneficial effect of internal pressure is more pronounced in the case of closing bending moments.

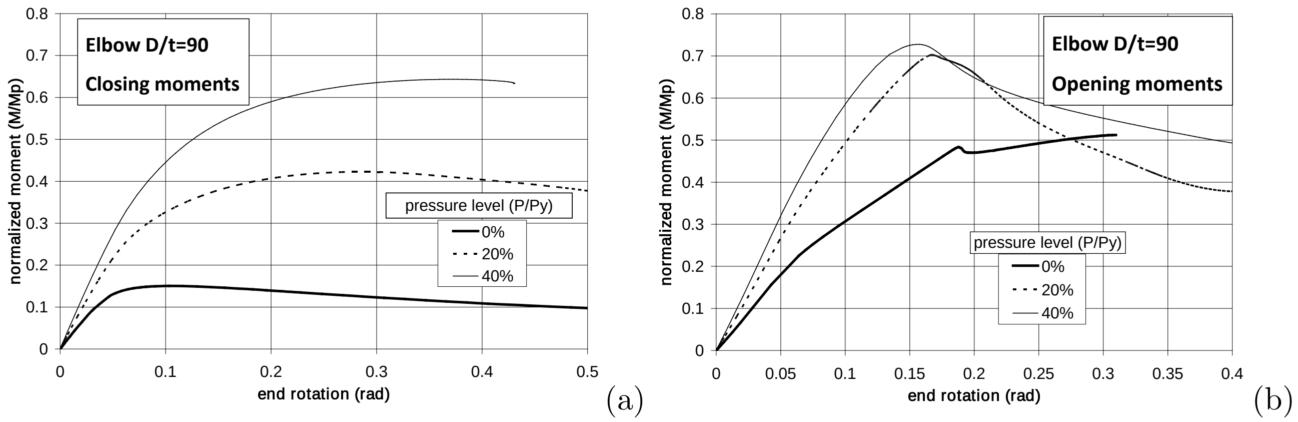

Figure 13. Response of a thin-walled 90 deg elbow (D/t=90) under in-plane opening bending, for three levels of internal pressure; (a) moment – rotation diagram and (b) ovalization – rotation diagram.

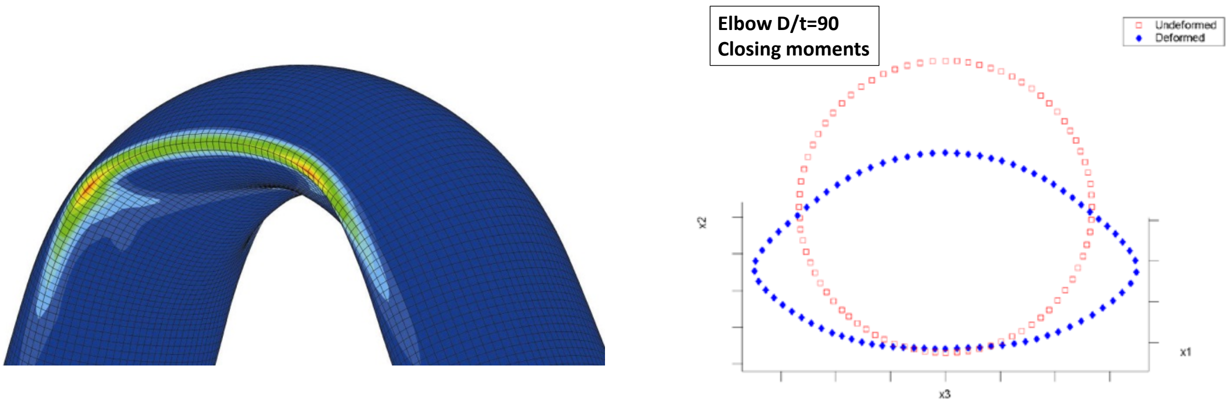

Figure 14. Thin-walled 90 deg elbow (D/t=90): deformed cross-sectional shapes and spread of plastic deformation under closing bending moments for zero pressure.

The response of a thick-walled 90-degree elbow under in-plane bending is shown in Figure 15a and Figure 15b for closing and opening bending moments, obtained numerically (Karamanos *et al.*, 2006). The pipe has diameter D=165 mm, thickness t=8.25 mm and bend radius R=480 mm. This response has similarities with the response of the thin-walled pipe elbow examined previously. Under closing bending moments, cross-sectional ovalization governs the response, leading to a limit moment, after which bending moment decreases. However, the ovalization shape, depicted in Figure 14b, is characterized by a "smoother" bending deformation at the flank locations, when compared with the corresponding shape of the thin-walled pipe elbow. The effects of internal pressure on the pipe bending response under closing moments is also characterized by an increase of bending moment capacity with increasing internal pressure, as shown in Figure 15a. This response has the same trends as the ones shown in Figure 13a for the thin-walled pipe (D/t=90). On the other hand, a reduction of bending moment capacity is observed for increased internal pressure levels in the case of opening bending moments (Figure 15b); in this case, due to the low value of the D/t ratio associated with very small ovalization, geometric effects are small and the elbow response is governed by plasticity. Therefore, the increase of internal pressure level results in early yielding and a decrease of the bending moment capacity.

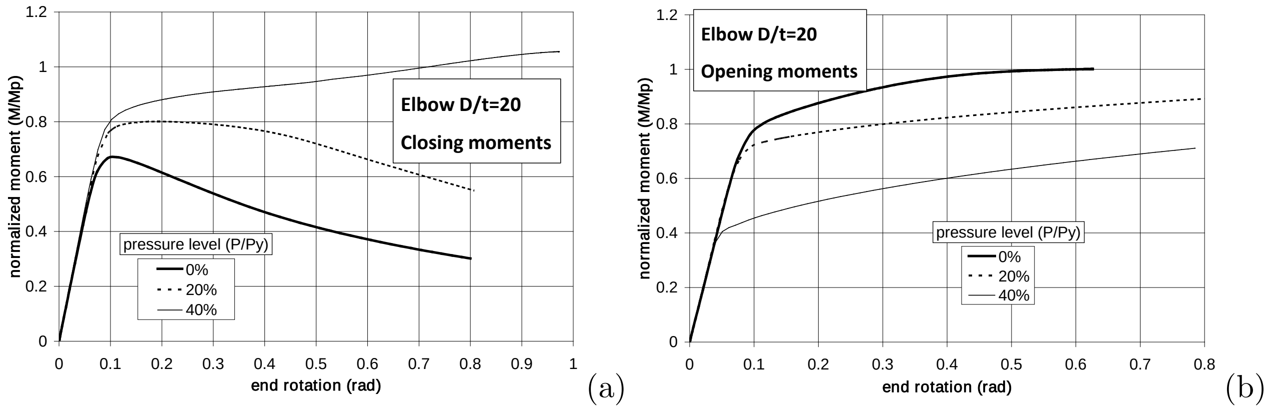

Figure 15. Response of 90 degree elbows under in-plane closing bending moments and three levels of internal pressure; (a) thin-walled elbow (D/t=90) and (b) thick-walled elbow (D/t=20).

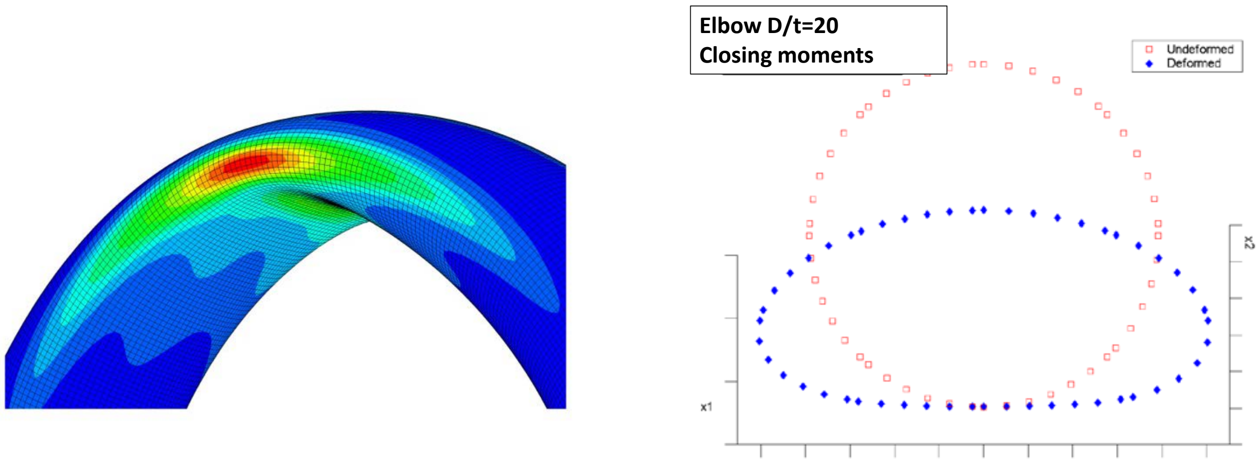

Figure 16. Deformed thick-walled elbow (D/t=20): cross-sectional shape and spread of plastic deformation under in-plane closing bending moments for zero pressure.

The response of a pipe bend under out-of-plane bending is an important aspect of pipe analysis, but has received less attention in the literature. Figure 17a shows the nonlinear response of a 90-degree elbow, subjected to out-of-plane bending, obtained both experimentally with the set-up of Figure 6 and numerically, using finite element simulations, as described in Karamanos *et al.* (2006). Note that cross-sectional ovalization is measured at the central section of the elbow, both experimentally and numerically, at an oblique direction of 45 degrees with respect to the plane of bending shown in Figure 17b, where maximum ovalization occurs (see Figure 3c). The shape of the deformed elbow subjected to out-of-plane bending is verified by the finite element simulation depicted in Figure 17c.

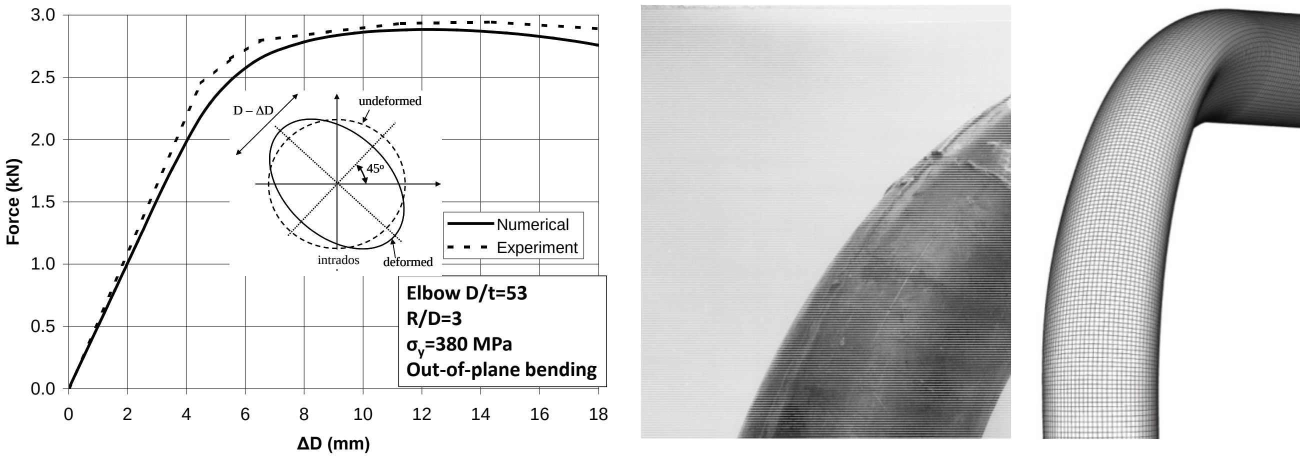

(a) (b) (c)

Figure 17. Out-of-plane loading of an elbow of moderate thickness (*D/t*=53); (a) force Q versus cross-sectional flattening at central cross-section and (b) deformed shape of specimen obtained experimentally and numerically.

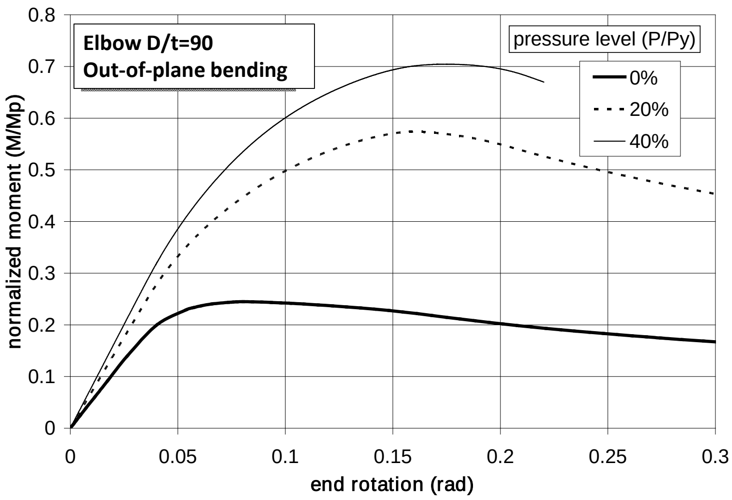

Figure 18. Response of a thin-walled 90 deg elbow (*D/t*=90) under out-of-plane bending moments and three levels of internal pressure (0, 20% and 40% of p_y)

The response of a thin-walled 90 deg elbow with *D/t* ratio equal to 90 under severe out-of-plane bending moments is shown in Figure 18, for three levels of internal pressure (0%, 20% and 40% of the yield pressure), and the corresponding pipe elbow shapes are shown in Figure 19. The results in Figure 18 indicate that the ultimate bending moment in the absence of internal pressure is well below the fully plastic moment of the pipe cross-section, and the corresponding failure mode is local buckling at the intrados of the pipe elbow, shown in Figure 19a (three-dimensional view) and in Figure 20a (cross-sectional view). The shape of the buckled elbow is characterized by small wavelength wrinkles in a 45-degree direction with respect to the plane of bending. One should notice that the application of out-of-plane bending moment, result in elbow torsion; a simple analysis of principal stresses in torsion, explains the oblique orientation of the wrinkles (Figure 21). In the presence of internal pressure, the out-of-plane bending moment capacity of the thin-walled pipe elbow is significantly increased. Furthermore, increase of internal pressure prevents the distortion of pipe cross-section, resulting in a "bulging" mode of buckling, depicted in Figure 19c for a pressure level equal to 40% of the yield pressure.

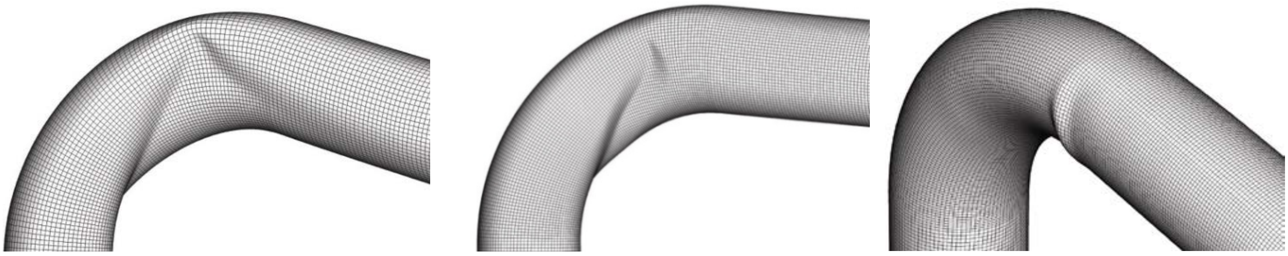

(a) (b) (c)

Figure 19. Buckled shapes of thin-walled 90 deg elbow (D/t=90) under out-of-plane bending moments for; (a) zero pressure, (b) pressure level 20% of p_y and (c) pressure level 40% of p_y.

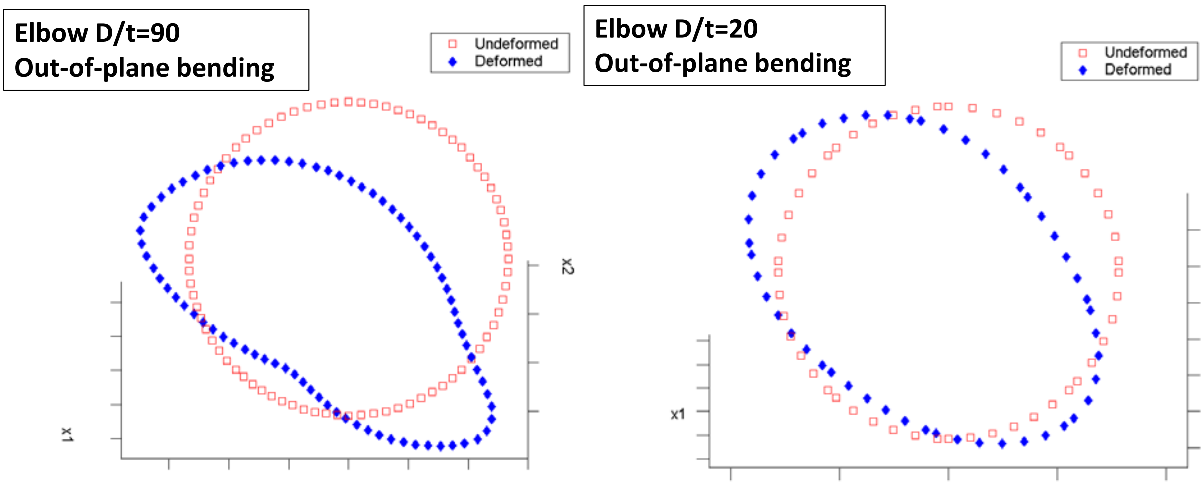

Figure 20. Deformed configuration of central cross-section under out-of-plane bending; (a) thin-walled elbow (D/t=90) and (b) thick-walled elbow (D/t=20).

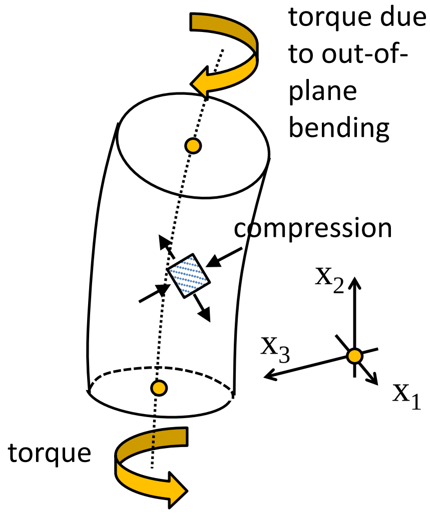

Figure 21. (a) Deformed shape of a 90 deg elbow under out-of-plane bending. (b) Schematic representation of the state of stress on an arbitrary location at the “intrados” of the curved pipe portion due to out-of-plane torque.

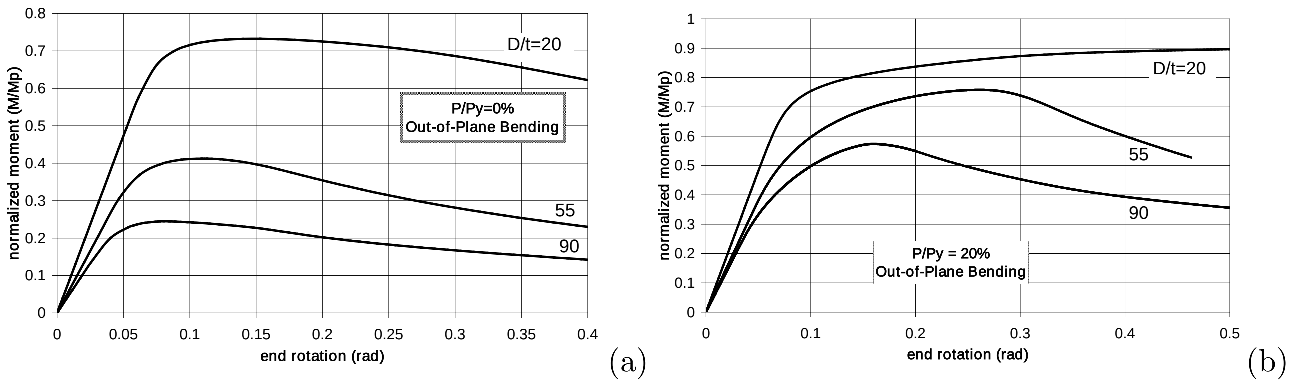

Figure 22. Response of elbows with D/t ratio equal to 20, 55 and 90, subjected to out-of-plane bending moments; (a) zero internal pressure; (b) pressure 20% of p_y.

The effect of pipe diameter-to-thickness ratio on pipe elbow under out-of-plane bending is shown in Figure 22 for zero pressure and pressure 20% of yield. The comparison for zero pressure in Figure 22a shows that thick-walled pipe elbows (D/t=20) may reach a maximum bending moment higher than 70% of the plastic moment, whereas the bending moment capacity of thinner elbows (D/t=55, 90) is significantly lower. In the presence of internal pressure, those differences are less pronounced, as shown in Figure 22b.

Pipe elbows are also used in offshore pipeline systems, such as “Christmas trees”, risers and manifolds (Kathayat *et al.*, 2012). In deep offshore applications, pipes are quite thick to resist high levels of external pressure. However, the combination of external pressure and bending loading may result in pipe failure. Despite the fact that the effects of those combined loading conditions on structural response and stability of straight pipe segments have been extensively investigated (Corona and Kyriakides, 1988; Karamanos and Tassoulas, 1991), mainly motivated by the installation process of deep water pipelines, the corresponding behaviour of offshore pipe elbows has received very little attention. Motivated by offshore pipeline applications, Bruschi *et al.* (2006) have presented an investigation of the mechanical behaviour of 32-inch-diamater pipe elbows with thickness equal to 1.1 *in*, D/t=30), and bend ratio R/D=5, without accounting for the effects of external pressure. To the authors' knowledge, the work presented by Pappa *et al.* (2008) has been the only attempt to investigate external pressure effects on onshore elbows, using numerical solution similar to the one reported by Karamanos *et al.* (2003, 2006). Figure 23 and Figure 24 shows the decrease of bending capacity of elbows, in the presence of external pressure, for both closing and opening bending moments.

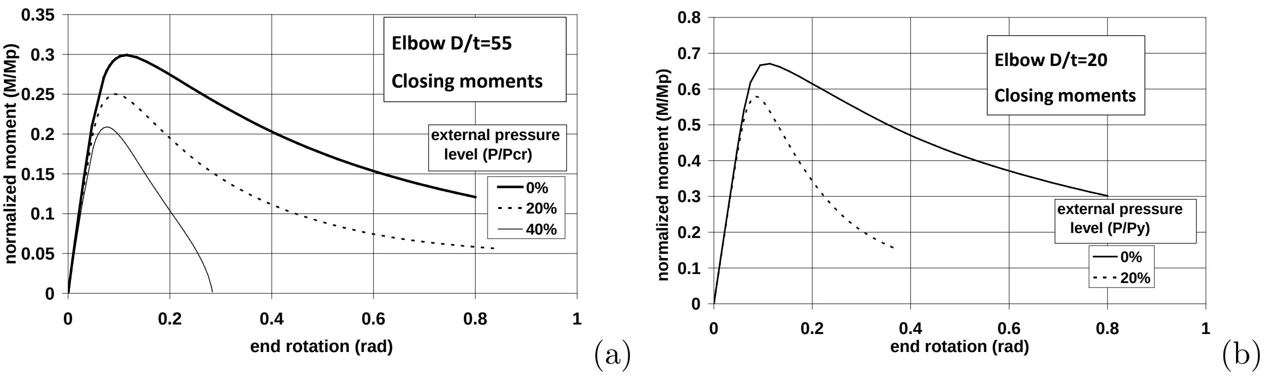

Figure 23. Moment – rotation diagram of elbows under in-plane closing bending in the presence of external pressure up to 40% p_y (D/t equal to 55 and 20).

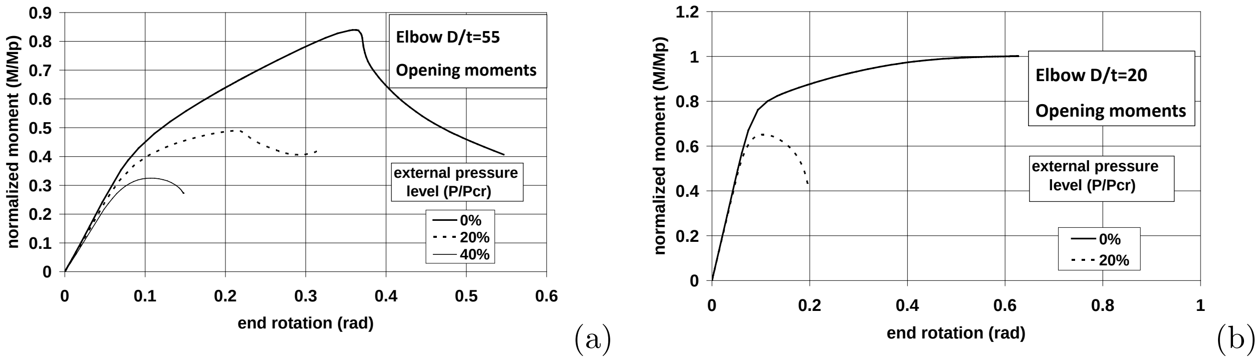

Figure 24. Moment – rotation diagram of elbows under in-plane opening bending in the presence of external pressure up to 40% p_y (D/t=55, 20).

4. Behavior under strong cyclic loading

Piping and pipeline systems are often subjected to strong cyclic loading, associated with repeated excursions of pipe material in the inelastic range, leading to fatigue damage. Pipe elbows have been identified as critical locations of those piping and pipeline systems, where fracture and loss of containment may occur due to low-cycle fatigue fracture. Under those cyclic loading conditions, the elbow may exhibit significant accumulation of plastic strain (often referred to as “ratcheting”), which eventually may lead to failure due to plastic collapse.

A significant part of the research associated with strong cyclic loading on elbows has been motivated by the seismic design and analysis of piping systems (Fujita *et al.*, 1978; Suzuki, 2006; Paolacci *et al.*, 2011). Extensive experimental work on the ratcheting behavior of pressurized 2-inch carbon and stainless steel pipe elbows has been reported by Yahiaoui *et al.* (1996a), under an “increasing input displacement amplitude” loading. This work was continued by Yahiaoui *et al.* (1996b) for out-of-plane bending, whereas Moreton *et al.* (1996) attempted to predict analytically the ratcheting rate and ratcheting initiation. Slagis (1998) reported an EPRI/NRC experimental testing program on carbon/stainless steel pipe elbows, through a shaking-table apparatus, for both component tests and piping system tests. Extensive experimental work was presented by Fujiwaka *et al.* (1999), through a series of material tests, pipe component tests and piping system tests (bent pipes, tees, and straight pipes).

DeGrassi *et al.* (2003) performed seismic time-history finite element analysis of piping system for simulating ratcheting, using the bilinear, multilinear and Chaboche models in

ANSYS. Balan and Redektop (2005) simulated the response of elbow specimen under cyclic bending and internal pressure with bilinear plasticity model in the finite element code ADINA. More recently, Rahman and Hassan (2009) presented an extensive analytical work on cyclic behavior of steel elbows, supported by 3 experiments on 2-inch SCH10 pipes, aiming at determining the capabilities of several cyclic plasticity models in predicting the ratcheting rate. All the above works demonstrated that when steel elbows are subjected to strong repeated loading, they present failure associated with material degradation or cyclic creep. In many instances, the elbow cross-section distorted or bulged with increasing number of cycles.

In the course of a large European research program (2009-2012), with acronym INDUSE (Pappa *et al.*, 2013), extensive research has been presented aimed at investigating the structural safety of industrial equipment structures and components under seismic loading with emphasis on process piping and elbows. More specifically, a series of experiments on pipe elbows under cyclic in-plane bending has been conducted, supported by numerical simulations. A first publication from this research effort, which included only numerical results, was reported recently (Varelis *et al.*, 2011), followed by a series of publications that reported both full-scale tests and numerical simulations (Varelis *et al.* 2013, 2015). It is important to notice that all the available data on cyclic loading of pipe elbows refer to in-plane bending loading, whereas there exist little information on test data and numerical simulations for cyclic loading under out-of-plane bending conditions.

Table 1 summarizes the experimental results reported in Varelis *et al.* (2013, 2015); 8-inch-diameter SCH40 long-radius steel pipe hot bends have been tested with nominal outer diameter and thickness equal to $D = 219.1$ mm and $t = 8.18$ mm respectively, and bend radius of the elbow equal to $R = 305$ mm under strong cyclic in-plane bending. The elbow configuration is shown in Figure 25a; it is composed by a 90-degree elbow fitting, attached to two straight pipe segments. The material of the specimens is P355N, according to EN 10216 standard, which is equivalent to API 5L X52 steel grade. Loading is imposed through the cyclic displacement of moving support supports, with amplitude Δl, as shown in Figure 25b, causing in-plane bending under repeated closing and opening conditions. A constant amplitude loading pattern has been applied on the specimens shown in Table 1, with the value of Δl ranged from ±25mm to ±300mm, with the exception of Test No. 8, where an increasing amplitude displacement is imposed. During the experiments, local strains have been measured, denoted as $\Delta\varepsilon_{H,exp}$.

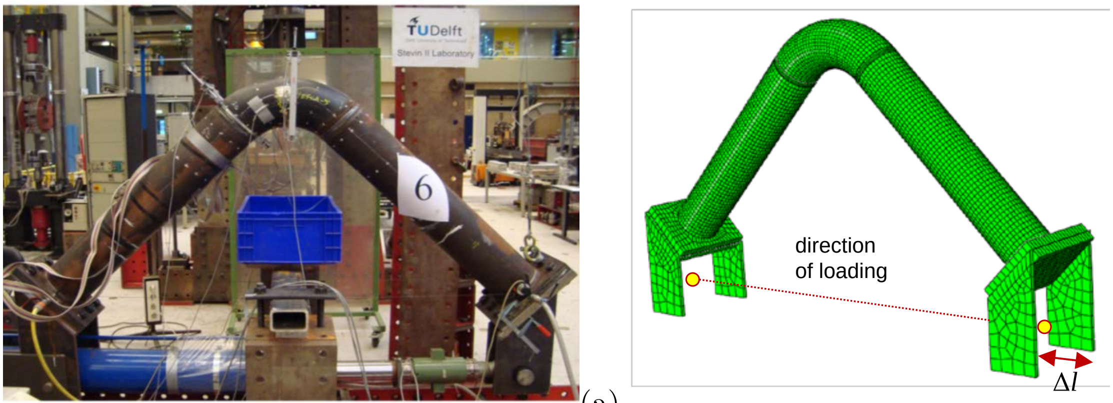

(a) (b)

Figure 25. In-plane bending loading of 8-inch-diameter elbows; (a) experimental set-up, (b) finite element model for numerical simulations (Varelis *et al.* 2013, 2015).

(a) (b) (c)

Figure 26. Failure of 8-inch-diameter SCH 40 elbows; (a) fatigue crack at elbow flank; (b) cross-sectional ovalization; (c) finite element simulation results.

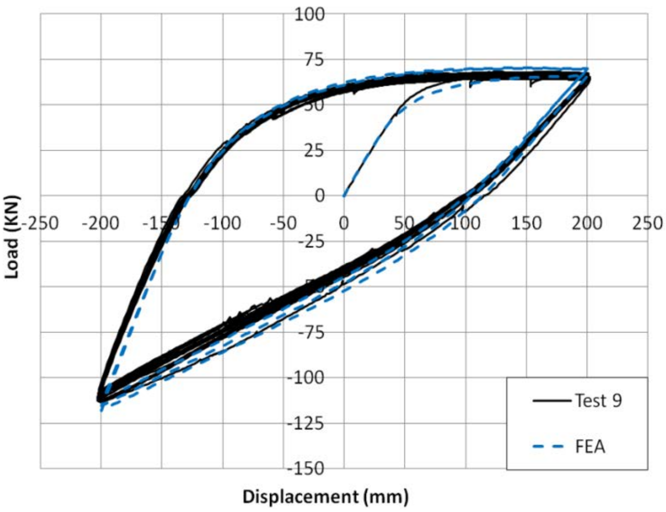

Figure 27. Load-displacement diagram for 8-inch-diameter SCH 40 (pressure 3.2 MPa, Δl=±200mm); comparison of test and numerical finite element results (Varelis and Karamanos (2015).

In those tests, both non-pressurized and pressurized, failure occurred in the form of a crack directed along the pipe axis at the flank location at the central cross-section of the pipe elbow, as shown in Figure 26a. The longitudinal direction of the crack indicates that fracture is due to excessive and repeated local strains in the hoop direction, due to cross-sectional ovalization, clearly shown in Figure 26b. This deformation is compatible with the deformed shapes of Figure 10a, Figure 11a, Figure 14.

In Figure 25b, a numerical finite element model that simulates the response of the pipe elbow under consideration is depicted (Varelis and Karamanos, 2015). The numerical results are compared with experimental results in Figure 26 in terms of the deformed shape, in Figure 27 in terms of the load-displacement diagram and in Table 1 in terms of the local strain variation in the hoop direction $\Delta\varepsilon_H$. In this Table, the strain variation in the longitudinal direction $\Delta\varepsilon_L$ is also shown, and its value is generally lower than the value of $\Delta\varepsilon_H$.

Test No.	Δl (mm)	N_f number of cycles	P pressure (MPa)	$\Delta\varepsilon_{H,exp}$ (%)	$\Delta\varepsilon_H$ (%)	$\Delta\varepsilon_L$ (%)
1	±25	13160	0.0	0.33	0.33	0.04
2	±70	444	0.0	1.23	1.25	0.14
3	±100	171	0.0	-	1.59	0.14
4	±150	61	0.0	2.61	2.55	0.16
5	±200	28	0.0	-	2.77	0.16
6	±250	17	0.0	3.84	3.75	0.18
7	±300	10	0.0	4.02	4.03	0.30
8	increasing amplitude	16	0.0	n/a		
9	±200	26	3.2	3.01	2.89	0.23
10	±300	10	3.2	-	2.39	0.97
11	±200	27	7.0	-	2.69	0.39
12	±300	10	7.0	1.94	2.25	0.98
13	±200	22	12.0	-	0.63	1.49

It is important to note that in obtaining reliable numerical results from the finite element simulations, the choice of the constitutive model is of primary importance. The constitutive model should be capable of describing accurately the response of steel material under cyclic loading conditions, and in particular: (a) the plastic plateau upon initial yielding, (b) the

Bauschinger effect upon reverse loading, and, (c) most importantly, the phenomenon of material ratcheting, i.e. the gradual accumulation of plastic deformation of the material, under constant-amplitude cyclic loading. Ratcheting has been observed in several experiments on cyclically-loaded elbows (Slagis, 1998; DeGrassi *et al.* 2003; Rahman and Hassan, 2009; Fenton and Hassan, 2014), characterized by a bi-axial state of strain, and constitutes a demanding simulation problem. For a thorough presentation of the challenges associated with bi-axial ratcheting the reader is referred to the recent works of Islam et al. (2015) and Hassan and Rahman (2015).

Using the finite element model shown in Figure 25b, Varelis and Karamanos (2015), simulation of ratcheting in cyclically-loaded elbows has been presented, using and the Tseng and Lee (1983) cyclic plasticity model, which is based on "two-surface" plasticity concept. The numerical results in Figure 28 indicated the accumulation plastic strain in the hoop direction, for the case of a non-pressurized elbow, comparing very well with experimental data. In addition, numerical calculations for the effects of pressure on hoop and longitudinal strain ratcheting at the critical location, is shown in Figure 29.

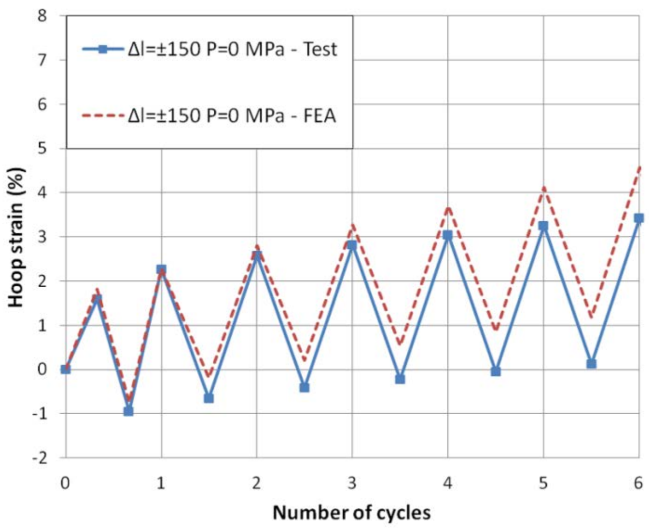

Figure 28. Accumulation of hoop strain (ratcheting) at the elbow critical location (flank); comparison between experimental and numerical results (Varelis and Karamanos, 2015).

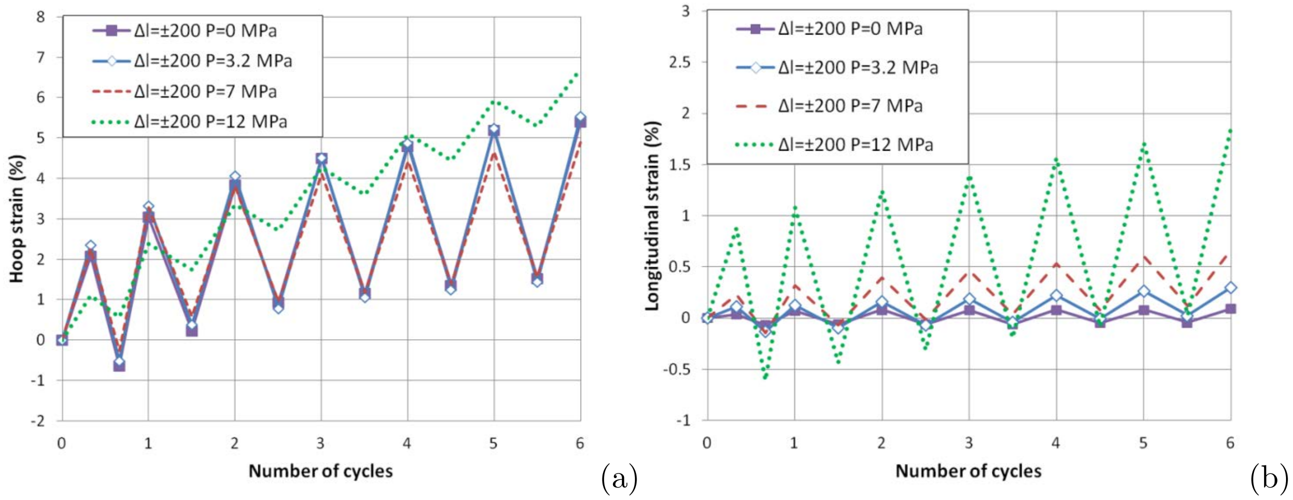

Figure 29. Pressure effects on the accumulation of longitudinal and hoop strain (ratcheting) at the elbow critical location (flank), obtained from numerical simulations (Varelis and Karamanos, 2015).

5. Behavior of buried pipeline bends

Steel transmission pipelines, in areas of significant geohazard areas (i.e. areas of significant seismic activity or areas of potential landslide risk), are subjected to severe permanent ground-induced actions, which may threaten the integrity of the buried pipeline. Pipeline ground-induced deformations are caused by tectonic fault action, liquefaction-induced lateral spreading, landslide movement, or soil subsidence, and may lead to pipeline failure, in the form of either local buckling in the form of a pipe wall wrinkling or pipe wall fracture due too excessive tensile strain.

This scientific area is receiving rapidly increasing attention during the last few years, considering that numerous large-diameter hydrocarbon pipelines are being constructed or planned for construction in geohazards areas. In the course of an efficient pipeline design and analysis under severe ground-induced actions, the deformation capacity of pipeline bends can be of particular importance. Several attempts have been published recently on the response of buried pipelines subjected to permanent ground deformations. However, all those works referred to straight pipeline segments and the effects of elbows has not been examined. To the author's knowledge, the only work on soil-pipe interaction that referred to pipe elbows is reported in the paper of Yoshizaki and Sakanoue (2004), but it focuses on lateral soil-structure interaction. In any case, the mechanical behavior of buried pipeline elbows is an open research issue, which requires more attention.

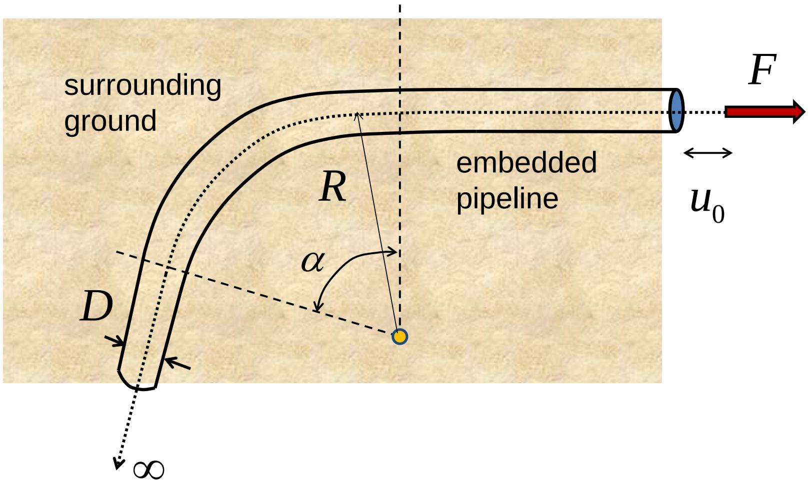

Figure 30. Schematic representation of a buried pipeline bend subjected to axial force.

The main feature of the response of buried pipeline elbows is the interaction of the deforming pipe with the surrounding soil. Figure 31 shows schematically a buried pipeline bend, subjected to axial tension in one end, while been infinitely long at the other end. Figure 31a shows a finite element model that represents the above physical problem. The model is similar to the models presented in (Vazouras *et al.*, 2010, 2012, 2015), and employs shell elements for modelling the pipeline, solid elements for modelling the surrounding soil and friction contact conditions for the soil-pipe interface. The steel pipeline under consideration has a 36 inch diameter, a thickness of ⅜ inch, and material grade X65 according to API 5L. The elbow is a 30-degree "hot bend" (α=30°), with bend radius parameter R/D equal to 5. The pipeline is pressurized at a level of 37.8 bar, which is 56% of the maximum design pressure. Two cohesive soils (clay) are considered for the surrounding ground conditions; Clay I is a soft-to-firm cohesive soil with cohesion 50 kPa and Young's modulus 25,000 kPa, whereas Clay II is a stiff cohesive soil with cohesion 200 kPa, Young's modulus 100,000 kPa. The pipe is subjected to an axial force F at the right end (Figure 31a), and it is considered to be infinitely long at the left end. The latter condition is enforced by the use of special-purpose nonlinear spring elements, which account for pipeline continuity to an infinite length, described in detail by Vazouras *et al.* (2015).

Figure 32 shows the response of the coupled soil-pipeline system, subjected to axial pull-out force F, for the 30 degree elbow. The load-displacement path is shown in Figure 32a and Figure 32b for the two soil conditions under consideration (Clay I and Clay II), together with the corresponding response of an infinitely long straight pipe, and the response of two other models, for a 60-degree elbow, and a 90-degree elbow respectively. The deformed configuration of the soil-pipe system is shown in Figure 31b and Figure 31c. The results in Figure 32 indicate that for the soil conditions under consideration, the response of buried pipeline elbows is more flexible than the response of a straight pipe with the same cross-sectional and material properties. This flexibility increases with the value of the bend angle, whereas stiffer soil conditions (Clay II) result in stiffer response. Currently, using the above numerical tools, extensive research is being conducted, towards (a) examining elbow integrity under severe ground-induced deformations and, more importantly, (b) investigating the use of the above flexibility property for mitigating fault crossing effects on buried pipelines.

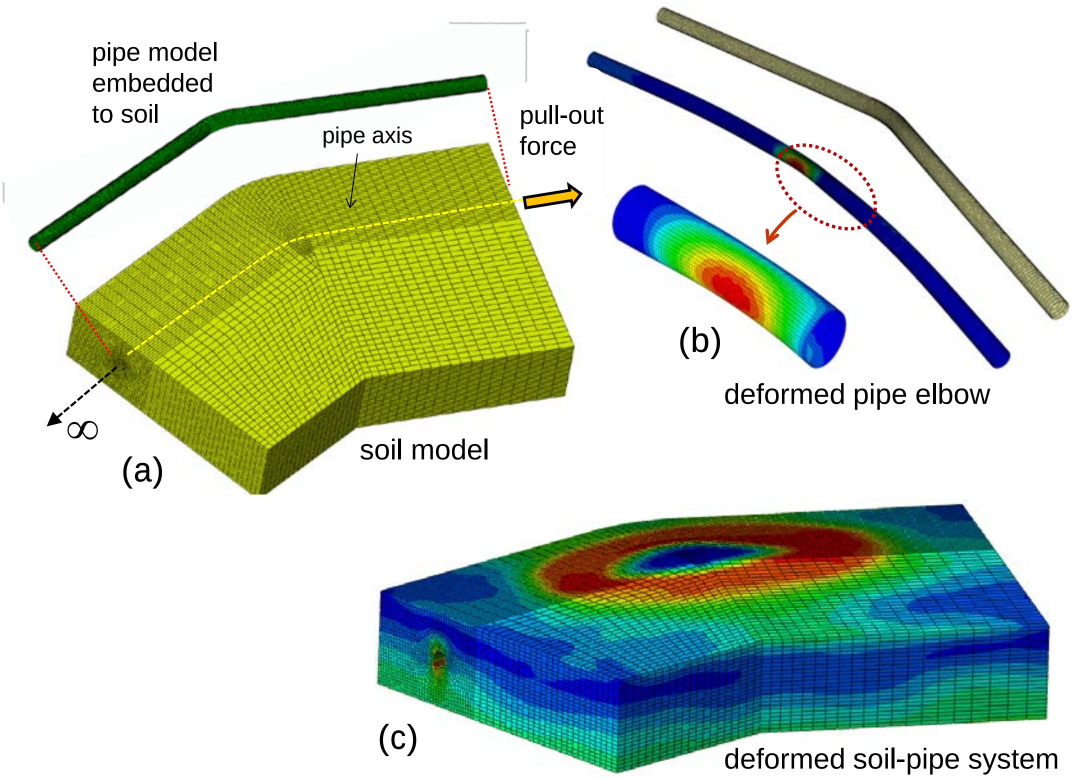

Figure 31. Coupled response of soil-pipeline system for a 30-degree bend subjected to axial (pull-out) force; finite element simulation.

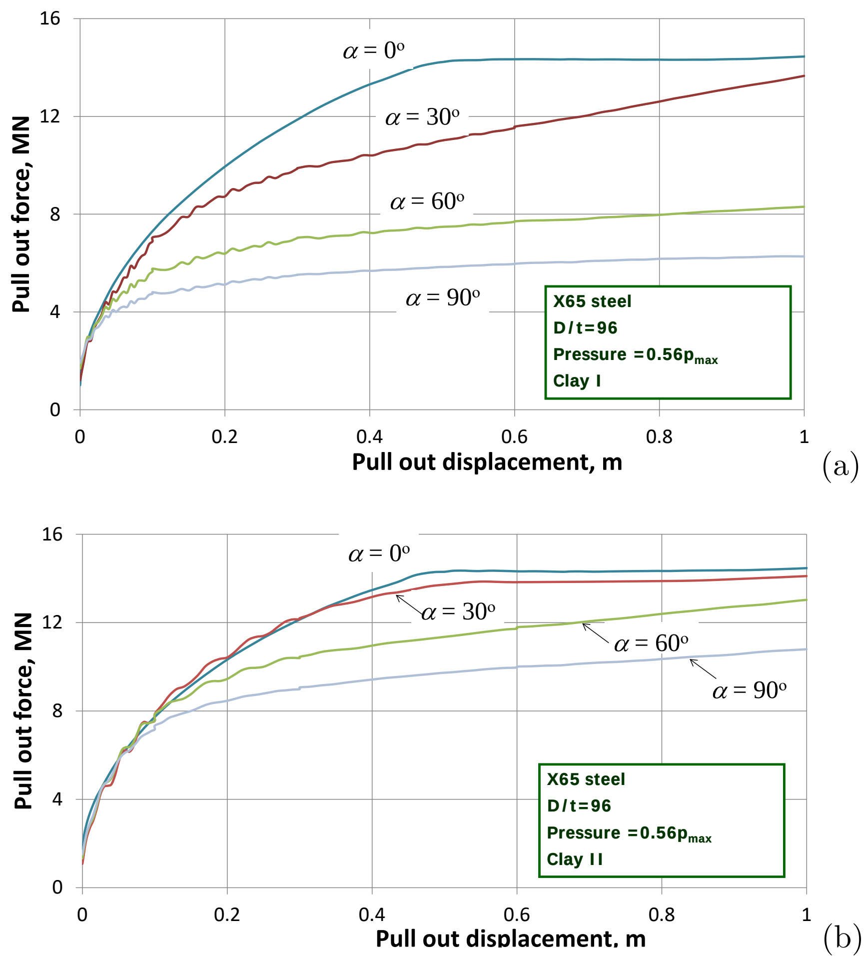

Figure 32. Pull-out force-displacement diagram for buried pipeline bends embedded in cohesive soil conditions; (a) soft-to-firm clay (Clay I); (b) stiff clay (Clay II).

6. Special-purpose elements for the numerical modelling of pipe elbows

In the course of piping and pipeline analysis, the numerical tools should be capable of describing accurately the significant cross-sectional deformation (distortion or "ovalization") of the elbow cross-section. Regular beam elements with circular cross-section, are inadequate to predict such a response, because they cannot describe the effects of pressure and – most importantly – the effects of cross-sectional ovalization on the mechanical response. On the other hand, the use of shell elements to discretize long segments of pipelines or piping systems is often computationally expensive for the purposes of pipeline design process, despite the rigorousness of such an approach. The above arguments have motivated the development and use of special-purpose elements, often referred to as "elbow", "pipe" or "tube" elements, as alternatives to shell elements. Those elements have several advantages over shell elements: their computational efficiency in terms of modelling and execution time, their convenience in applying boundary conditions at several cross-sections and kinematic constraints restraining in-plane and warping degrees of freedom, and the fact that the results from such special-purpose elements are more easily interpreted.

These special-purpose elements combine longitudinal (beam-type) deformation of the tube axis with cross-sectional deformation of the cylindrical tube wall. The first attempt to combine those two deformation modes in a simple and efficient tube element was described in the papers by Bathe and Almeida (1980, 1982). The element is based on the classical von Karman solution of elbow bending, and uses a simplified version of cylindrical linear theory for inextensional cross-sectional in-plane (no-warping) deformation, which is discretized through a series of trigonometric functions. The work of Bathe & Almeida (1980, 1982), was the first to distinguish longitudinal (beam-type) deformation from cross-sectional ovalization and couple them in a simple and efficient manner in the finite element formulation. Militello and Huespe (1988) proposed a further improvement of the above element considering including warping deformation, but keeping the inextensionality condition, using Hermite polynomials. In a more recent paper, Yan *et al.* (1999) have proposed an "enhanced pipe elbow element", which further improves the above concepts and capabilities. Their element allowed for warping deformation, and accounted for a certain degree of cross-sectional extensionality and for non-symmetric cross-sectional deformation. A special-purpose "elbow" element, incorporated in finite element program ABAQUS, has been developed for the elastic-plastic analysis of initially straight and bent tubes under pressure and structural loads, described in section 3.9.1 of ABAQUS Theory Manual (Simulia, 2015). The element is based on the Koiter – Sanders linear shell kinematics and on a discrete Kirchhoff concept, imposed through a penalty formulation. Cross-sectional warping is also included and the corresponding deformation parameters are discretized through the use of trigonometric functions up to the 6^{th} degree. Finally, special-purpose "tube" elements have also been developed by the author to investigate the nonlinear and buckling analysis of steel tubulars under structural loads and pressure, motivated by the structural behaviour of tubular members in deep offshore platforms (Karamanos and Tassoulas, 1996) The elements process three nodes on the tube axis, and cross-sectional deformation is described at each node on the basis of classical ring theory (Brush and Almroth, 1975), extended to include warping. Cross-sectional deformations (in-plane and warping) at every node are discretized using trigonometric functions, while the cross-sectional deformation parameters at each node as well as the nodal displacements and rotations are interpolated through the use of appropriate Lagrangian polynomials. Using an expansion up to the 16^{th} degree, those elements, incorporated in nonlinear analysis framework, have provided excellent results for the response of straight pipes and pipe bends, compared with experimental data, and in particular, the simulation of local buckling.

Inclusion of pressure effects (internal or external) in those special-purpose elements is of particular importance for the accurate prediction of pressurized pipe elbows. Pressure is not a regular surface load; it is a distributed follower load, always normal to the pipe surface and, therefore, further adjustments are required on the stiffness matrix of the pipe. Among other contributions, aimed at describing those effects on the pipe stiffness matrix, one may notice the paper by Hibbit (1979), which has been used extensively in several commercial programs.

The capabilities of such elements in predicting pipe elbow behaviour is shown in Figure 8, where the results from the "tube element", introduced by Karamanos and Tassoulas (1996), compare very well with shell element calculations and the experimental results. In addition to the moment-rotation diagram, the "tube element" analysis is capable of predicting local buckling and describing post-buckling behaviour, similar to the one depicted in Figure 10b or Figure 11b. For more information on this issue, the reader is referred to the paper by Karamanos *et al.* (2003). These results demonstrate that special-purpose elements, if properly used, they can simulate the behaviour of piping systems and pipelines with a good level of accuracy.

7. Conclusions

Pipe bends (elbows) are critical components for the structural integrity of piping systems and pipelines. Because of their geometry, under structural loading, they are more flexible in comparison with straight pipes having the same cross-sectional and material properties, exhibiting significantly higher stresses and deformations.

Under extreme loading conditions, pipe elbows may undergo substantial cross-sectional ovalization. In-plane closing bending moments result in failure due to flattening in a direction perpendicular to the plane of bending. The corresponding bending moment capacity is quite low with respect to the fully-plastic moment of the pipe cross-section. In the case of opening bending moments, the response is characterized by "reverse ovalization", resulting in higher bending moment capacity, and failure occurs in the form of local buckling. The response under out-of-plane bending moments is characterized by cross-sectional ovalization in an oblique direction with respect to the plane of bending. The effect of internal pressure is generally positive, due to its stabilizing effect that prevents both ovalization and local buckling. However, for the particular case of thick-walled elbows subjected to opening bending moments, those geometric effects are minimal, plasticity governs the response and the presence of internal pressure reduces the bending capacity. Finally, numerical simulations on rather thick-walled pipe elbows, candidates for offshore pipeline applications, indicate that the presence of external pressure reduces the bending moment capacity.

Pipe elbows subjected to severe cyclic loading, may fail due to low-cycle fatigue. Based on a series of experiments on elbows under in-plane bending, supported by numerical simulations, fracture occurs at the elbow flank due to cyclic "folding" of the area because of ovalization. The level of internal pressure did not modify the mode of failure, and did not affect significantly the number of cycles to failure. Ratcheting of local strains at critical locations has also been detected both experimentally and numerically. It is also noticed that there is a lack of tests on elbows under out-of-plane bending cyclic loading.

The mechanical response of buried pipeline elbows is a topic that requires further investigation. Their response is characterized by soil-pipeline interaction and soil conditions have a significant effect on pipeline elbow deformation. Numerical results for cohesive soil conditions, obtained through a rigorous finite element model, demonstrate that the response of pipe elbows is more flexible than the response of straight pipes with the same cross-sectional and material properties, and this flexibility increases with the value of the bend angle.

Finally, a short note on special-purpose elements for modelling pipes and elbows is offered. Those elements have been developed as alternatives to shell elements, combine longitudinal deformation with cross-sectional ovalization and, if properly used, they are capable of describing the mechanical response of elbows under pressure and structural loading with a good level of accuracy.

Acknowledgements

A significant part of the work presented in this paper has been supported during the period 2009-2014 by the Research Fund for Coal and Steel (RFCS), under research grants RFSR-CT-2009-00022 (program INDUSE) and RFSR-CT-2011-00027 (program GIPIPE). The author would like to thank in particular ir. Arnold M. (Nol) Gresnigt, Associate Professor at TU Delft, The Netherlands, Dr. George E. Varelis, Senior Engineer at PDL Solutions (Europe) Ltd, Hexhan, UK, Dr. Polynikis Vazouras, Research Associate at the University of Thessaly and Mrs. Patricia Pappa, Research Assistant at the University of Thessaly. Finally, the continuous support of the Seismic Engineering Technical Committee of ASME PVPD since 2004, is greatly appreciated.

References

American Society of Mechanical Engineers, 2007, *Factory-Made Wrought Buttwelding Fittings*, B16.9, ASME Code for Pressure Piping, New York, NY.

American Society of Mechanical Engineers, 2010a, *Power Piping*, B31.1, ASME Code for Pressure Piping, New York, NY.

American Society of Mechanical Engineers, 2010b, *Process Piping*, B31.3, ASME Code for Pressure Piping, New York, NY.

Balan, C. and Redekop, D., 2005, "The effect of bidirectional loading on fatigue assessment of pressurized piping elbows with local thinned areas.", *International Journal of Pressure Vessels and Piping*, 82, pp. 235-242.

Bathe, K.-J. and Almeida, C. A., 1980, "A simple and effective pipe elbow element – linear analysis.", *Journal of Applied Mechanics*, ASME, Vol. 47, pp.93-100.

Bathe, K.-J. and Almeida, C. A. 1982, “A simple and effective pipe elbow element – interaction effects.”, *Journal of Applied Mechanics*, ASME, Vol. 49, pp.165-171.

Bruschi, R., Barbas, S., Mandke, J., Bartolini, L. M., and Vitali, L., 2006, “Deformation capacity of induction bends.”, *25th International Conference on Offshore Mechanics and Arctic Engineering*, OMAE 2006-92241, Hamburg, Germany.

Brush, D. O. and Almroth, B. O., 1975, *Buckling of bars, plates and shells*, McGraw Hill, New York, NY.

Chattopadhyay J., Nathani, D. K., Dutta, B. K. and Kushwaha, H. S., 2000, “Closed-Form Collapse Moment Equations of Elbows Under Combined Internal Pressure and In-plane Bending Moment.”, *Journal of Pressure Vessel Technology*, ASME, Vol. 122, pp. 431-436.

Comité Européen de Normalisation, 1999, *Butt-welding pipe fittings – Part 1: Wrought carbon steel for general use and without specific inspection requirements*, Standard EN 10253-1, Brussels.

Comité Européen de Normalisation, 2002, *Metallic industrial piping - Part 3: Design and calculation*, Standard EN 13480-3, Brussels.

Corona, E. and Kyriakides, S., 1988, “On the collapse of inelastic tubes under combined bending and pressure.”, *International Journal of Solids and Structures*, Vol. 24, pp. 505-535

DeGrassi, G., Hofmayer, C., Murphy, A., Suzuki, K., and Namita, Y., 2003, “BNL nonlinear pre-test seismic analysis for the NUPEC ultimate strength piping test program.”, *Transactions of SMiRT 17 Conference*, Prague, Czech Republic.

Dhalla, A. K., 1987, “Collapse Characteristics of a Thin-Walled Elbow.”, *Journal of Pressure Vessel Technology*, ASME, Vol. 109, pp. 394-401.

Fenton, M., and Hassan, T., 2014, "Low-Cycle Fatigue Failure Responses of Short and Long Radius Elbows.", *Pressure Vessels and Piping Conference*, ASME PVP2014-28805.

Fujita, K., Shiraki, K., Kitaide, K. and Nakamura, T., 1978, “Vibration damage experiment of the curved pipes (elbows) relating to seismic ultimate strength.”, *Transactions of The Japan Society of Mechanical Engineers*, Vol. 44, No. 386, pp. 3437-3445 (in Japanese).

Fujiwaka, T. Endou, R., Furukawa, S., Ono, S., and Oketani, K., 1999, “Study on strength of piping components under elastic-plastic behavior due to seismic loading.”, *Pressure Vessels and Piping Conference,* PVP-Vol 137.

Greenstreet, W. L., 1978, *Experimental Study of Plastic Responses of Pipe Elbows*, ORNL/NUREG-24 report, Contract No. W-7405-eng-26.

Gresnigt, A. M. *et al.*, 1985, “Preofresultaten van Proeven op Gladde Bochten en Vergelijking Daarvan met de in OPL 85-333 Gegeven Rekenregels.”, [in Dutch], *Institute for Construction Materials and Structures*, TNO-IBBC, Report OPL 85-334, Delft, The Netherlands.

Gresnigt, A. M., 1986, “Plastic Design of Buried Steel Pipelines in Settlement Areas.”, *Heron*, Vol. 31, No. 4, Delft, The Netherlands.

Gresnigt, A. M. and van Foeken, 1995, “Strength and Deformation Capacity of Bends in Pipelines.”, *Int. J. Offshore and Polar Engineering*, Vol. 5, No. 4, pp. 294-307.

Hassan T., and Rahman S. M., 2009, “Simulation of Ratcheting Responses of Elbow Piping Components.”, *Pressure Vessels and Piping Conference*, ASME PVP2009-77819.

Hassan, T., and Rahman, S. M., 2015, "Constitutive Models in Simulating Low-Cycle Fatigue and Ratcheting Responses of Elbow.", *Journal of Pressure Vessel Technology*, Vol. 137, No.3.

Hibbit, H. D., 1979, “Some follower forces and load stiffness.”, *International Journal for Numerical Methods in Engineering*, Vol. 14, No.6, pp. 937-941.

Hilsenkopf, P., Boneh, B. and Sollogoub, P., 1988, “Experimental Study of Behavior and Functional Capability of Ferritic Steel Elbows and Austenitic Stainless Steel Thin-Walled Elbows.”. *International Journal of Pressure Vessels and Piping*, Vol. 33, pp. 111-128.

Islam, N., Fenton, M., and Hassan, T., 2015, "Long and Short Radius Elbow Experiments and Evaluation of Advanced Constitutive Models to Simulate the Responses.", *Pressure Vessel and Piping Conference*, ASME, PVP2015-45688, Boston, MA.

Kathayat, T. S., Hill, R. T., Goyal, R. K., and Dhar, S., 2012, “Behaviour of Mechanical Properties of High Wall Thickness and Grade in Hot Induction Bending.”, OTC 22906, *Offshore Technology Conference*, Houston, Texas.

Karamanos, S. A. and Tassoulas. J.L., 1991, “Stability of inelastic tubes under external pressure and bending.”, *Journal of Engineering Mechanics,* ASCE, Vol. 117, pp. 2845-2861.

Karamanos, S. A. and Tassoulas, J. L., 1996, “Tubular Members I: Stability Analysis and Preliminary Results.’, *Journal of Engineering Mechanics*, ASCE, Vol. 122, No. 1, pp.64-71.

Karamanos, S. A., Giakoumatos, E. and Gresnigt, A. M., 2003, “Nonlinear Response and Failure of Steel Elbows Under In-Plane Bending and Pressure.”, *Journal of Pressure Vessel Technology*, ASME, Vol. 125, No. 4, pp. 393-402.

Karamanos, S. A., Tsouvalas, D. and Gresnigt, A. M., 2006, “Ultimate Bending Capacity and Buckling of Pressurized 90 deg Steel Elbows.”, *Journal of Pressure Vessel Technology*, ASME, Vol. 128, No. 3, pp. 348-356.

Millittelo, C. and Huespe, A. E., 1988, “A displacement-based pipe elbow element.”, *Computers and Structures*, Vol. 29, No.2, pp. 339-343.

Moreton, D.N., Yahiaoui, K., and Moffat, D.G., 1996, “Onset of ratchetting in pressurised piping elbows subjected to in-plane bending moments.”, *International Journal of Pressure Vessels and Piping*, Vol. 68, No. 1, pp. 73-79.

Mourad, H. M. and Younan, M. Y. A., 2001, “Nonlinear analysis of pipe bends subjected to out-of-plane moment loading and internal pressure.”, *Journal of Pressure Vessel Technology*, ASME, Vol. 123, No. 2, pp. 253-258.

Mourad, H. M. and Younan, M. Y. A., 2002, “Limit-load analysis of pipe bends under out-of-plane moment loading and internal pressure.”, *Journal of Pressure Vessel Technology*, ASME, Vol. 124, No. 1, pp. 32-37.

Paolacci, F., Reza, M. S., and Bursi, O. S., 2011, “Seismic design criteria of refinery piping systems.”, COMPDYN 2011, *Conference on Computational Methods in Structural Dynamics and Earthquake Engineering*, Corfu, Greece.

Pappa, P., Tsouvalas, D., Karamanos, S. A. and Houliara, S., 2008, “Bending Behavior of Pressurized Induction Bends.”, *Offshore Mechanics and Arctic Engineering Conference*, ASME, OMAE2008-57358, Lisbon, Portugal.

Pappa, P. *et al.*, 2013, *Structural Safety of Industrial Steel Tanks, Pressure Vessels and Piping Systems under Seismic Loading*, INDUSE RFCS project, Final Report, Brussels; available in http://bookshop.europa.eu.

Rahman, S. M. and Hassan, T., 2009, “Simulation of ratcheting responses of elbow piping components.”, *Pressure Vessel and Piping Conference*, ASME, PVP2009-77819, Prague, Czech Republic.

Rodabaugh, E. C., and George, H. H., 1957, “Effect of internal pressure on the flexibility and stress intensification factors of curved pipe or welding elbows.”, *Transactions of the ASME*, Vol. 79, pp. 939-948.

Shalaby, M. A. and Younan, M. Y. A., 1998, “Limit Loads for Pipe Elbows with Internal Pressure Under In-plane Closing Bending Moments.”, *Journal of Pressure Vessel Technology*, ASME, Vol. 120, pp. 35-42.

Shalaby, M. A. and Younan, M. Y. A., 1999, “Effect of Internal Pressure on Elastic-Plastic Behavior of Pipe Elbows Under In-plane Opening Bending Moments.”, *Journal of Pressure Vessel Technology*, ASME, Vol. 121, pp. 400-405.

Simulia, 2011, *Abaqus Theory Guide*, ABAQUS software, version 6.11, Dassault Systèmes Simulia Corp., Providence, RI, USA.

Slagis, G. C., 1998, "Experimental Data on Seismic Response of Piping Components.", *Journal of Pressure Vessel Technology*, ASME, Vol. 120, pp.449-455.

Sobel, L. H. and Newman, S. Z., 1980, "Comparison of Experimental and Simplified Analytical Results for the In-Plane Plastic Bending and Buckling of an Elbow.", *Journal of Pressure Vessel Technology*, ASME, Vol. 102, pp. 400-409.

Sobel, L. H. and Newman, S. Z., 1986, "Simplified, Detailed and Isochronous Analysis and Test Results for the In-Plane Elastic-Plastic and Creep Behavior of an Elbow.", *Journal of Pressure Vessel Technology*, ASME, 108, pp. 297-304.

Suzuki, K., 2006, "Earthquake Damage to Industrial Facilities and Development of Seismic Vibration Control Technology – Based on Experience from the 1995 Kobe Earthquake.", *J. Disaster Research*, Vol. 1, No.2.

Suzuki, N. and Nasu, M., 1989, "Non-Linear Analysis of Welded Elbows Subjected to In-Plane bending.", *Computers and Structures*, Vol. 32, No.3/4, pp. 871-881.

Tan, Y., Matzen, V. C. and Yu, L. X., 2002, "Correlation of test and FEA results for the nonlinear behavior of straight pipes and elbows", *Journal of Pressure Vessel Technology*, ASME, Vol. 124, pp. 465-475.

Tseng, N. T. and Lee, G. C., 1983, "Simple plasticity model of the two-surface type.", *Journal of Engineering Mechanics*, Vol. 109, pp. 795-810, ASCE.

Varelis, G. E., Pappa, P., and Karamanos, S. A., 2011, "Finite element analysis of industrial steel elbows under strong cyclic loading.", *Pressure Vessel and Piping Conference*, ASME, PVP2011-57260, Baltimore, Maryland, USA.

Varelis, G. E., Karamanos, S. A., and Gresnigt, A. M., 2013, "Steel Elbow Response Under Strong Cyclic Loading.", *Journal of Pressure Vessel Technology*, ASME, Vol. 135, No.1, Article Number: 011207.

Varelis, G. E., and Karamanos, S. A., 2015, "Low-Cycle Fatigue of Pressurized Steel Elbows Under In-Plane Bending.", *Journal of Pressure Vessel Technology*, ASME, *Vol.* 137, No.1, Article Number: 011401.

Vazouras, P., Karamanos, S. A., and Dakoulas, P., 2010, "Finite Element Analysis of Buried Steel Pipelines Under Strike-Slip Fault Displacements.", *Soil Dynamics and Earthquake Engineering*, Vol. 30, No. 11, pp. 1361–1376.

Vazouras, P., Karamanos, S. A., and Dakoulas, P., 2012, "Mechanical Behaviour of Buried Steel Pipelines Under Strike-Slip and Normal/Reverse Fault Displacements.", *Soil Dynamics and Earthquake Engineering*, Vol. 41, pp. 164-180.

Vazouras, P., Dakoulas, P., and Karamanos, S. A., 2015, "Pipe-Soil Interaction and Pipeline Performance Under Strike-Slip Fault Movements.", *Soil Dynamics and Earthquake Engineering*, Vol. 72, pp. 48–65.

Von Karman, T., 1911, "Uber die Formuanderung dunnwandiger Rohre." [in German], *Zeit. Des Vereines deutcher Ingenieure*, Vol. 55, pp. 1889-1895.

Yahiaoui, K., Moffat, D.G., and Moreton, D.N., 1996, "Response and cyclic strain accumulation of pressurized piping elbows under dynamic in-plane bending.", *Journal of Strain Analysis for Engineering Design*, 31 (2), pp. 135-151.

Yahiaoui, K., Moreton, D.N., and Moffat, D.G., 1996, "Response and cyclic strain accumulation of pressurized piping elbows under dynamic out-of-plane bending.", *Journal of Strain Analysis for Engineering Design*, 31 (2), pp. 153-166.

Yan, A. M., Jospin, R. J. and Nguyen, D. H., 1999, "An enhanced pipe elbow element – Application in plastic limit analysis of pipe structures.", *International Journal for Numerical Methods in Engineering*, Vol. 46, pp. 409-431.

Yoshizaki K. and Sakanoue T., 2004, "Analytical Study on Soil-Pipeline Interaction due to Large Ground Deformation.", *13th World Conference on Earthquake Engineering*, Paper No. 1402, Vancouver, Canada.